EPA-R2-72-099

68-02-0309/4-72

IN-STACK TRANSMISSOMETER TECHNIQUES FOR MEASURING OPACITIES OF PARTICULATE EMISSIONS FROM STATIONARY SOURCES

by

Carl M. Peterson, Ph.D.
M. Tomaides, Ph.D.
ENVIRONMENTAL RESEARCH CORPORATION
3725 North Dunlap Street
St. Paul, Minnesota 55112

Prepared for

ENVIRONMENTAL PROTECTION AGENCY
National Environmental Research Center
Division of Chemistry and Physics
Research Triangle Park,
North Carolina 27711

Contract No. 68-02-0309
April 1972

IN-STACK TRANSMISSOMETER TECHNIQUES FOR MEASURING OPACITIES OF PARTICULATE EMISSIONS FROM STATIONARY SOURCES

by

Carl M. Peterson, Ph.D.
M. Tomaides, Ph.D.
ENVIRONMENTAL RESEARCH CORPORATION
3725 North Dunlap Street
St. Paul, Minnesota 55112

Prepared for

ENVIRONMENTAL PROTECTION AGENCY
National Environmental Research Center
Division of Chemistry and Physics
Research Triangle Park,
North Carolina 27711

Contract No. 68-02-0309
April 1972

ABSTRACT

Field studies were conducted to obtain basic research data as a base for developing design and performance specifications for transmissometers which are to be used to measure smoke stack plume opacities. Tests, conducted on the stack of a pulverized coal-fired power plant, were designed to evaluate the influence of transmissometer illumination and light receiving angles, and transmitted light wavelength on in-stack opacity measurements and their correlation with the stack plume opacity.

Two specially-designed transmissometers, one having a small fixed illumination-viewing angle design and the other having adjustable illumination and viewing angles, were mounted on a cylindrical 145-inch diameter steel stack to measure the in-stack opacity. A 0.5° telephotometer was used to determine the out-of-stack opacity of the plume as viewed from a distant river bank.

The results show a significant dependence of measured in-stack transmittance as a function of illumination and receiver angles. This dependence is most pronounced at small angles. The measured transmittance increases with increasing illumination and viewing angle, resulting in 5 and 46 percent errors for 5° and 60° angles, respectively, when compared to true transmittance. The dependence of measured transmittance as a function of illumination light wavelength was also established.

Using a small fixed illumination-viewing angle design transmissometer, a good correlation was obtained between plume opacity and in-stack transmittance.

This report was submitted in fulfillment of Contract 68-02-0309 under the sponsorship of the Environmental Protection Agency.

CONTENTS

FIGURES

FIGURES (continued)

TABLES

SECTION I

CONCLUSIONS

The major conclusions drawn from the test results are:

1. The apparent transmittance of an aerosol as measured by a transmissometer increases with the size of the transmitter and receiver angles of the transmissometer. This is due to the increase in the amount of scattered light detected by the transmissometer as these angles increase in size. Detection of scattered light by a transmissometer represents an error in the measurement and should be minimized as much as possible.

2. The measured transmittance can be singly influenced by varying either the receiver or transmitter angle and both these angles are nearly equally influential in effecting the measured transmittance within 0-60°.

3. A positive error of about 5 percent was noted when 5° receiver and transmitter angles were employed for transmittance measurements of a pulverized coal-fired boiler effluent. The error increased to about 46 percent when 60° receiver and transmitter angles were employed. The tests were conducted with an experimental transmissometer using a tungsten lamp, a photoelectric detector, and a light beam diameter (aperture size) of approximately four inches.

4. The transmittance of the pulverized coal-fired boiler effluent studied was light wavelength dependent. A difference from 6 to 10 percent in transmittance was measured when employing interference filters of 0.438 to 0.656 micron. The 0.656 micron filter (red band) consistently provided the lowest in-stack transmittance. This result would indicate that the particles in the effluent were sufficiently large to exceed the first maximum of the particle extinction curve and/or significant spectral absorption effects were present.

5. Good agreement was found between the opacity of the plume and the in-stack transmittance of the coal-fired boiler emission. For high transmittance conditions (greater than 70 percent) ideal agreement was observed between remote plume transmittance measurements by telephotometry of contrasting targets in back of the plume and in-stack transmittance measurements by a transmissometer with a 3° receiving angle, 1.5° transmitter angle, and a tungsten lamp light

diameter of 0.5 inch. For lower transmittance conditions (less than 40 percent), the in-stack measurement was approximately 4 percent higher. The error may be due to an increase in the particle size and/or multiple scattering effects at low transmittance. In either case, the error would probably be reduced by employing a smaller receiving angle.

SECTION II

RECOMMENDATIONS

This program was limited to field tests performed at one facility. It was not within the scope of the program to extensively evaluate optical properties of fly ash under varying size distribution and concentration as related to the opacity measurement. It is recommended, however, that such testing be carried out.

As found during tests, the measured value of in-stack opacity depends strongly on the transmissometer illumination and viewing angles. It may also be dependent on the light beam diameter used for the aerosol illumination. Tests, or at least theoretical calculations, should be carried out to evaluate the influence of this common design parameter.

SECTION III

INTRODUCTION

Since the turn of this century, a number of theorists have concerned themselves with fundamental studies to explain, predict or calculate the extinction and scattering of a beam of light passing through a suspension of fine particles or intercepting a single particle. Coincident with such studies has been the development of methods, techniques and instruments to measure the magnitude of such phenomena.

As a result, it is now possible to specify with reasonable certainty the optical conditions for extinction and scattering measurements in systems of particles of undetermined shape, size and composition, and to anticipate what quantitative information about the particles can be deduced from such measurements. Hodkinson[1] has clearly and concisely presented a review and critique of the noted activity, described methods of applying the evolved principles to achieve suitable measurements and quantitatively interpreted results of his and fellow investigators. Conner and Hodkinson[2] have discussed in detail the optical properties and visual effects of smoke-stack plumes.

Properly measured and interpreted optical properties of plumes can be related to the quantity and quality of material contained in a plume. Capable of being interpreted in such a manner, a measure of the optical properties can be used to indicate the effectiveness of system processes, applied control equipment and malfunction in controls.

One of the basic plume optical properties is its optical transmittance which is defined as the ratio of light flux which reaches a light sensitive device (eye, photocell, etc.) when the flux from the source passes through the plume and when it does not. The basic equation is given by Equation (1):

$$T = \frac{F}{F_o} = \exp(-naQt) \qquad (1)$$

where

T = transmittance

F = flux of transmitted light through plume

F_o = maximum flux of light measured in absence of plume in line of source and sensor

n = the number of particles per unit volume of air in the light path of length t through the aerosol

a = the projected area of one of these particles

Q = the particle extinction coefficient or efficiency factor defined as:

$$Q = \frac{\text{total flux scattered and absorbed by a particle}}{\text{flux geometrically incident on the particle}}$$

The particle extinction coefficient or extinction efficiency factor Q depends on the particle refractive index relative to the surrounding medium, its shape and its size relative to the wavelength usually expressed as $\alpha = \pi d/\lambda$, where d is the particle diameter and λ is the wavelength of light in the medium surrounding it; α is termed a particle size parameter.

Another property of the plume is its opacity which is a measure of the light flux attenuated by the plume that can be calculated from the transmittance as per Equation (2):

$$O = 1-T \qquad (2)$$

The optical density (OD) of the same plume is expressed as the logarithm of the transmittance or opacity as per Equation (3):

$$OD = -\log_{10}T = -\log_{10}(1-O) \qquad (3)$$

From the discussion and results presented by Conner and Hodkinson,[2] a remote method of measuring plume opacity by means of contrasting targets is described. Actually, this is a calculated plume transmittance value (T_p) obtained by Equation (4):

$$T_p = \frac{B_s' - B_h'}{B_s - B_h} \qquad (4)$$

B_s and B_s' are the luminance measured by focusing with a telephotometer on a specific target (sky) respectively clear and through the plume. B_h and B_h' are the luminance obtained when focusing on a second target (hill) respectively clear and through the plume. Performed in this manner, a defineable plume transmittance or opacity is obtained. It is this value upon which the plume opacity is judged and compliance to most control regulations is based. Therefore, if in-stack transmittance measurements are to be of value for determining plume opacity, they must be relatable to such plume measurements. A significant difference between plume and in-stack opacity measurements may be realized in the fact that the effective path length may be different. In-stack opacity readings can be reduced in practice to the plume opacity by use of Equation (5):

$$\log_{10}(1-O_1) = (\ell_1/\ell_2) \log_{10}(1-O_2) \qquad (5)$$

where

O_1 = plume opacity

O_2 = in-stack opacity

ℓ_1 = stack exit or plume diameter

ℓ_2 = in-stack transmissometer path length.

SECTION IV

OBJECTIVES

A number of in-stack transmissometers are commercially available for the continuous monitoring of in-stack gas transmittance. However, due to the absence of defined operation and performance specifications, there has been little standardization in design of such instruments with regard to illuminating and receiving angle, wavelength of illumination, sensitivity and type of receiver, and relationship of output to plume opacity. Environmental Protection Agency (EPA) officials and users have questioned the accuracy and meaning of the data generated by such an array of uniquely-designed transmissometers. It was, therefore, the object of this study to answer these questions by developing an experimental transmissometer with extensive research flexibility and collect and interpret data from such a unit while operating it on a coal-burning electric power plant stack.

The experimental transmissometer employed was flexible enough in design and the effluent stack gases were of adequate quality to determine the following:

1) The effect of transmitter and viewing angles on the measurement of transmittance;

2) The dependence of illuminating wavelength on the measurement of transmittance; and

3) The relationship between in-stack transmittance and plume opacity as a function of in-stack path length.

This report contains a description of the transmissometers employed in the study, the experimental test program applied, and the results achieved.

SECTION V

INSTRUMENTATION

Two in-stack transmissometers (a reference and an experimental model) were designed, developed and employed in this study to achieve the results reported. The reference model was designed with small fixed transmitter and receiver angles and was used to continuously monitor the transmittance of gases flowing from the boiler to the atmosphere. The experimental model was designed with sufficient flexibility to permit changes to be made in the transmitter and viewing angles and also to accommodate various interference filters. All other equipment used in the course of the program activity was commercially available.

Reference Transmissometer

The reference transmissometer consists of a transmitter and a receiver. In operation the transmitter is mounted on one wall of a duct or stack and is the source of illumination. The receiver is mounted directly opposite the transmitter and functions to measure that portion of the radiant energy which is transmitted through the gas flowing within the confines of the stack boundaries.

Schematics of the reference transmitter and receiver are shown in Figures 1 and 2, respectively. The basic support and housing for each is a rigid 3-inch I.D. aluminum tube, flat-black anodized to eliminate excessive light reflection. Within this tube and at defined separation distances, as shown in the figures, are located the proper lens, pin holes and photocell. The support tube was of sufficient internal diameter so that all internal items can be first mounted within an independent holding fixture. At two points (diametrically opposite) and near the circumference of each fixture, provisions were made to accept a quarter-inch rod and locking set-screw. Two quarter-inch rods were then attached to the first fixture and serially extended through each succeeding fixture. The distance between fixtures was readily measured and held in this position by tightening the locking set-screws. The entire optical assembly was then positioned in the support tube as shown in Figures 1 and 2.

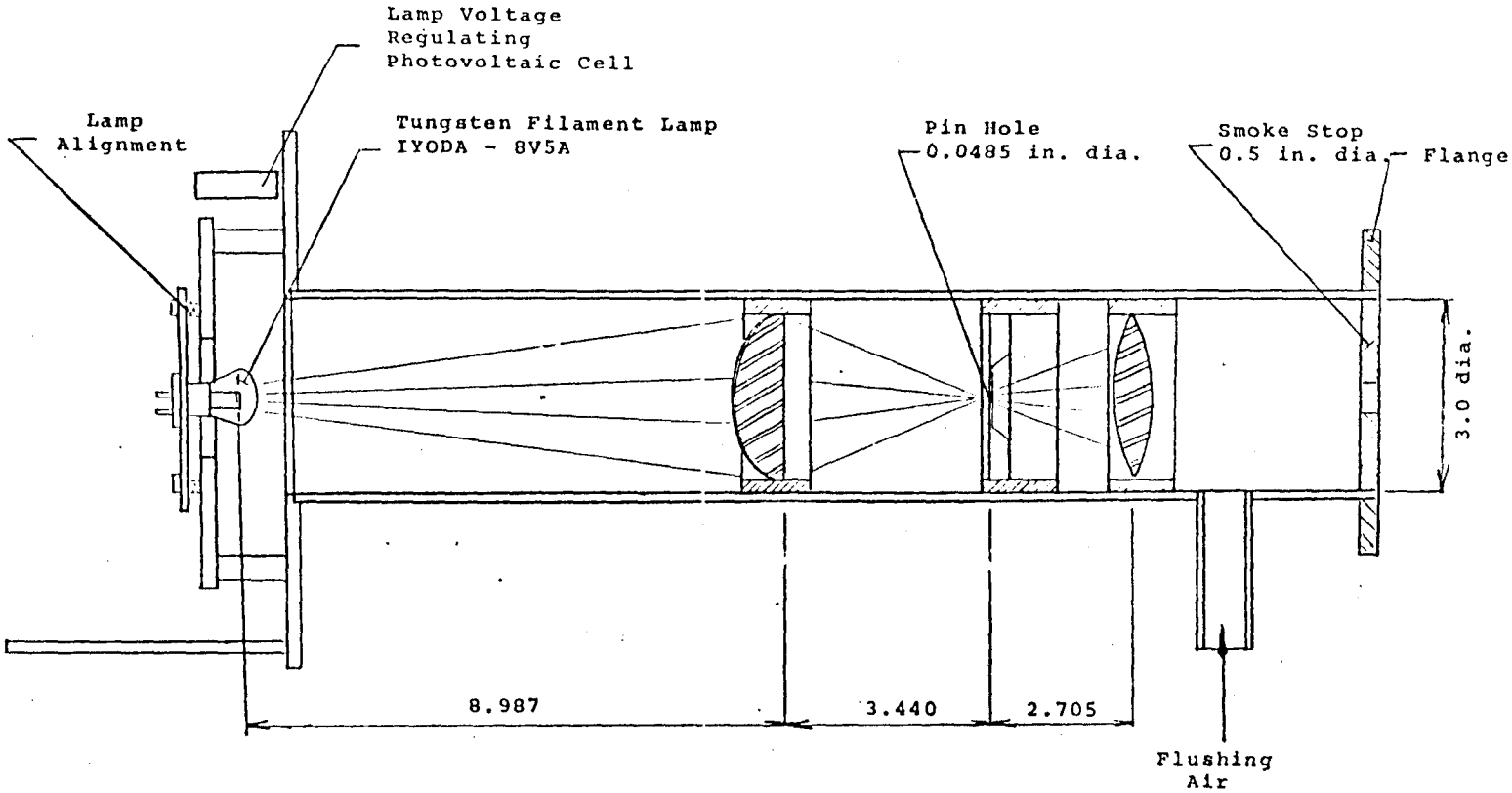

Figure 1. Schematic and Basic Dimensions of the Reference Transmissometer Transmitter.

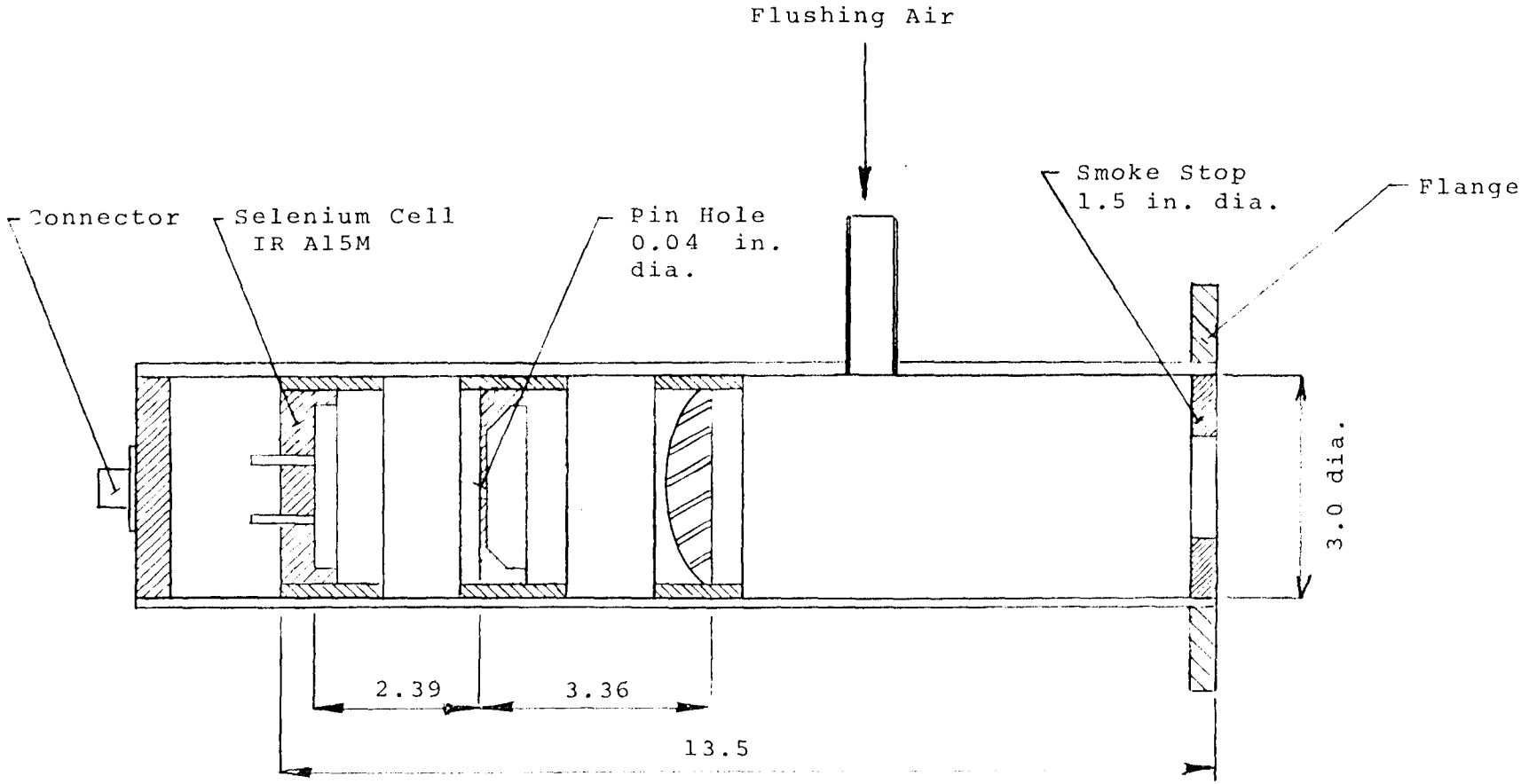

Figure 2. Schematic and Basic Dimensions of the Reference Transmissometer Receiver.

As shown in Figure 1, the transmitter optical assembly consists of a Tiyoda 8V5A square-shaped filament lamp, two lenses, and a pinhole of 0.0485-inch diameter. The optical system is protected against dust deposits by introducing clean flushing air between the first lens and the stack. A smoke stop is an integral part of the support tube which terminates in a flange used for attaching the assembly to the stack wall.

The optical assembly tube and the illumination lamp are mounted to a rigid frame to secure optic alignment during instrument operation or transportation. This frame also encompasses the electronic components of the instrument and is entirely enclosed in an aluminum housing with a removable cover for the convenience of electronic circuitry adjustment and maintenance. Complete assembly of the reference transmissometer transmitter is shown in Figure 3.

The optical portion of the reference receiver is designed to be assembled in the same manner as the transmitter. The receiver consists of a single lens protected from dust deposits by a clean air ventilated smoke stop, followed by a pinhole and a IR A15M selenium cell surface. The electronic system of the transmitter/receiver is located in the transmitter housing and performs two functions: it provides a stabilized voltage to the lamp; and conditions the photocell output signal. The wiring diagram for this device is included as Appendix B of this report.

The stabilized lamp voltage power supply maintains the Tiyoda 8V5A lamp at a nominal 6.5 volts. The lamp intensity is continuously monitored and adjusted for fluctuations and aging by a secondary photocell which is part of a feedback circuitry of the power supply.

The electrical signal-conditioning circuitry consists of a temperature-stabilized solid-state amplifier. The electrical signal is received at the conditioning circuit from the receiver through a shielded weatherproof cable and, after proper conditioning, is suitable for 0-10 millivolt recorder operation. Electrical jacks are provided on the transmitter housing for continuously recording the conditioned signal.

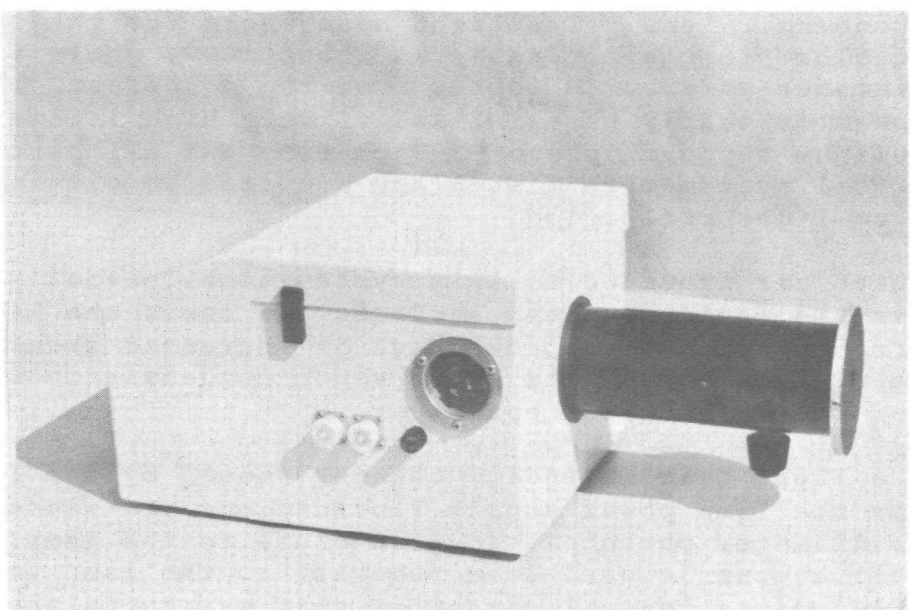

Figure 3. Photograph of the Reference Transmitter Assembly.

Experimental Transmissometer

The separated transmitter and receiver concept was also applied to the experimental transmissometer design.

Several techniques for varying the transmitter and receiver angle of transmissometers were investigated and the final design selected is shown in Figure 4. The experimental transmissometer contains a lamp (Tiyoda 8V5A) which can be moved along the transmitter support tube axis, and the light from the lamp is collected by a 5-inch diameter condenser lens. The light beam angle for the lamp located close to the condenser is about 100°; while for a lamp distance of about 6 inches from the condenser, the light beam is nearly parallel and of very high intensity. The aluminum support tube of 3-inch I.D. and all parts of the optical system were flat-black anodized to eliminate excessive light reflection.

The sheath air provided to this system simultaneously protects the condenser lens surfaces and cools the lamp. This arrangement has the advantage of increased sheath air temperature which prevents water vapor condensation in front of the transmitter condenser.

Possible light beam intensity changes caused by the lamp aging or the lamp power supply fluctuations are sensed by a small diameter photocell located close to the lamp. The photocell output is used as a feedback to the lamp power supply automatic control circuitry that maintains the light intensity constant. The photocell temperature is stabilized to within ±0.5°F by a small wire resistor which is located in the photocell mount. The temperature is sensed by a thermistor which operates a Rosemount Temperature Controller STO-21501 that functions to control the energy to the resistor.

Similarly to the reference transmitter, the experimental transmitter is also enclosed in an aluminum housing and provided with power and low voltage shielded cord sockets. The transmitter lamp voltage can be conveniently checked on two outside terminals and adjusted to the voltage desired upon removing the housing cover. The light beam angle can be adjusted and the angle determined on a scale readable through a small opening on the side of the transmitter housing. The opening is sealed with a removable cover when

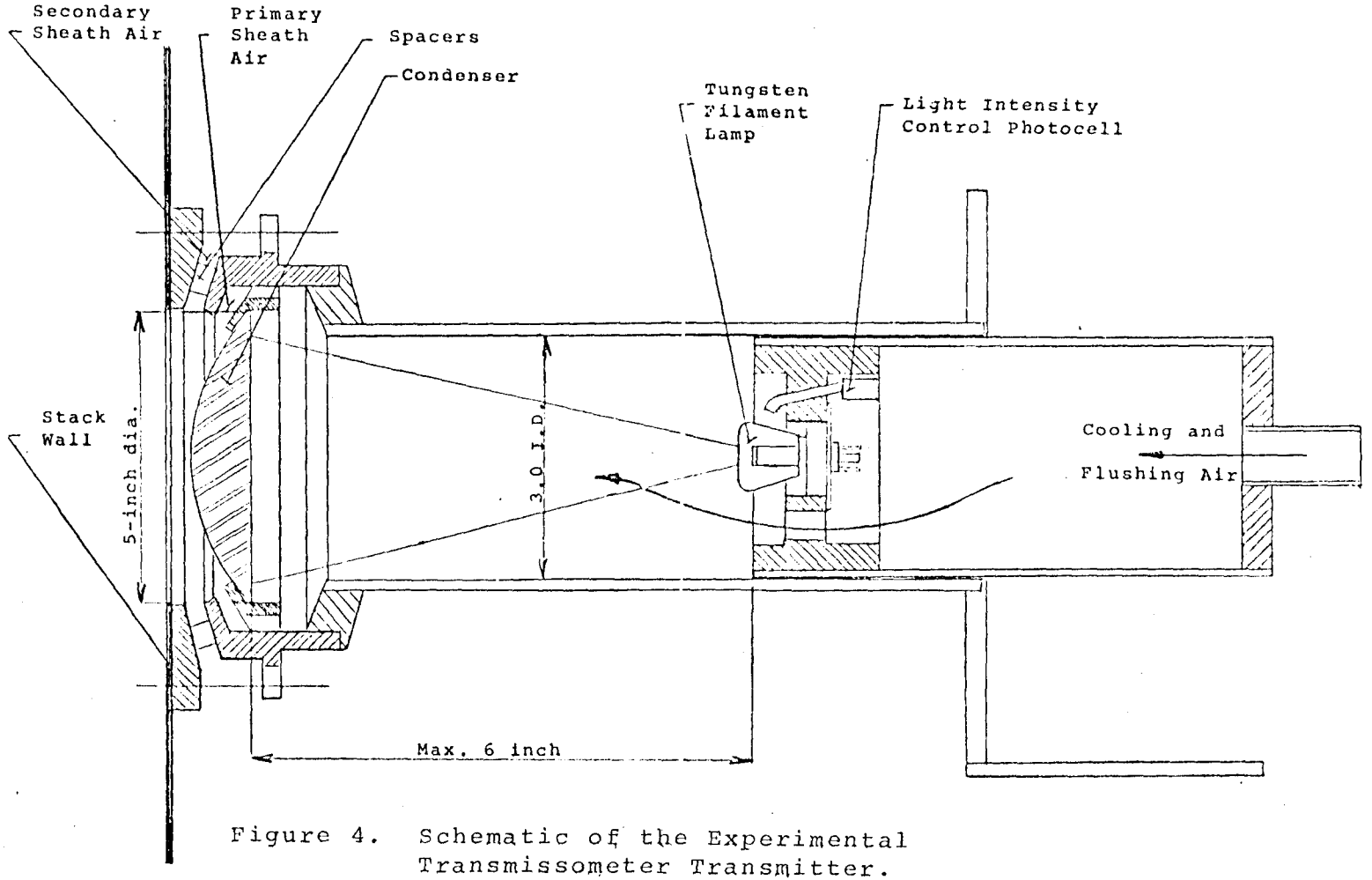

Figure 4. Schematic of the Experimental Transmissometer Transmitter.

in use. As calibrated, the transmitted light angle can be varied within near parallel zero degree angle up to 100 degrees. The lamp power supply located in the transmitter aluminum housing is of the same design as for the reference transmitter; however, for the experimental transmitter, a nominal lamp voltage of 8.0 volts was employed.

The final experimental transmissometer receiver design is shown in Figure 5. It contains a double aspheric objective lens that collects the light from the illuminated section of the stack at angles from about 110 degrees down to 2 degrees. The exact angle is dependent on the iris opening that is positioned between the objective and the light focusing lens. As a light sensing device, a photovoltaic cell A15M is used in connection with low noise solid-state signal pre-amplifier, which increases the total signal amplification of the secondary amplifier located in the transmitter housing by 10 and 100. The photovoltaic cell is temperature-stabilized by the Rosemount Temperature Controller STO-21501. The objective lenses are protected by flushing air supplied behind the smoke stop of the receiver.

The electronic circuitry of the experimental transmissometer is shown in Appendix B.

Auxiliary Equipment

A telephotometer, Spectra Brightness Spot Meter Model SB (0.5° type) by Photo Research Corporation, was used to determine the plume opacity. The technique used in this determination was that of contrasting targets.

A set of calibrated interference filters supplied by Optic Technology, Inc. was used to evaluate spectral behavior of the transmissometers. The specific major peak transmittance for each of five respective filters was 436, 486, 579 and 656 millimicron.

Two sources of clean air to protect the optical systems were constructed. Each source consists of a small blower and an absolute filter located in a metal box. Electrical heaters with proportional thermostatic control could be

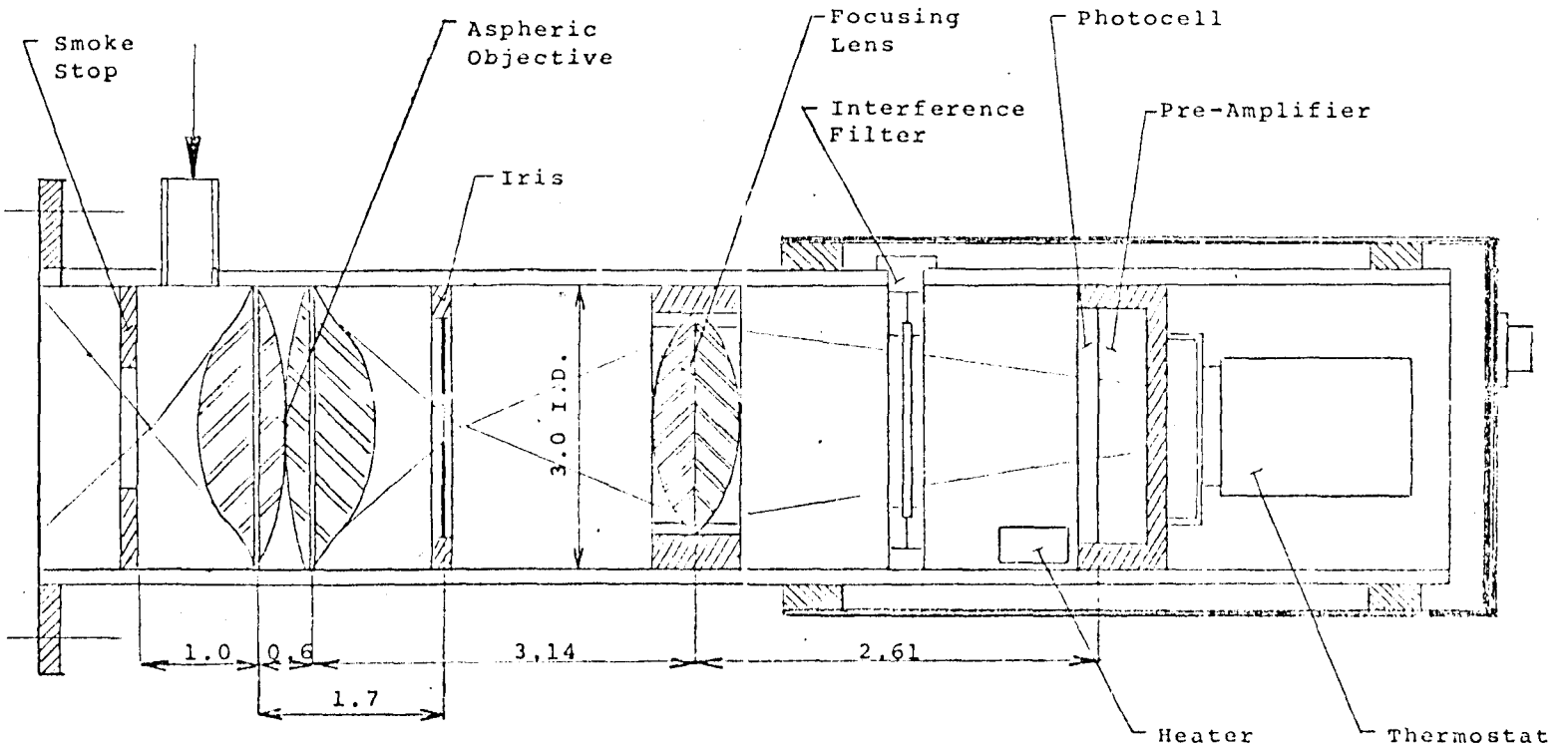

Figure 5. Schematic of the Experimental Transmissometer Receiver.

installed in each assembly if high temperature flushing sheath air were required. Air flow rate for each source was about 7 cfm.

Two Bausch & Lomb VOM-5 single channel strip chart recorders were used for simultaneous monitoring of the experimental and reference transmissometer signals.

SECTION VI

LABORATORY EVALUATION OF INSTRUMENTS

Functions of the instruments were checked and the transmissometers calibrated in the laboratory before collecting any field experimental data. The attention was mainly centered on the calibration of the reference and experimental transmissometer output when instruments were set to an optical path equal to the diameter of the stack. For each transmissometer the amplifier linearity was determined and the experimental transmitter and receiving angle scale factors were established. The data collected during laboratory calibration were used to calculate the accuracy and reproducibility of both transmissometers.

Reference Transmissometer

The reference transmissometer of 1.5° fixed transmitter angle was designed and used throughout the experiments. The receiver component was first operated and evaluated in the laboratory with a 3° receiving angle but later, when in-stack transmittance data showed a strong dependence on the magnitude of the receiver angle, the design changes were made to decrease the angle of view down to about 0.8°.

To determine the instrument sensitivity the entrance of the receiver was shielded and the amplifier output read at the so-called "dark current" condition. The output voltage as measured with a Keithley solid-state electrometer was within 0.0002 to 0.0003 volts. This value represents the minimum accuracy of the photovoltaic cell amplfier readout.

Based on this calibration the minimum detectable transmittance can be calculated. When the receiver and transmitter were optically aligned and the transmitter lamp operated at 6.5 volts, the receiver signal corresponding to clean air conditions and light path of 10 feet was 0.24 volts and for a 30-foot distance, 0.0357 volts. Supposing the amplifier output reading of 0.002 volts has an accuracy of ±0.0002 volts, that is ±10 percent, then the transmittance determined with the same accuracy would be:

$$T = \frac{0.002 \times 100}{0.0357} = 5.6 \text{ percent for 30 ft distance}$$

and

$$T = \frac{0.002 \times 100}{0.2400} = 0.83 \text{ percent for 10 ft distance.}$$

The accuracy in measurement improves rapidly with increasing transmittance and since the transmittance values below twenty percent are not anticipated or considered allowable during normal stack emission rates, the performance is considered to be acceptable.

The voltage stability of the photocell amplifier was determined by step-wise varying the amplifier input line voltage from 115 to 100 volts. No detectable change in amplifier output was detected. The drift of the amplifier during startup was less than 0.5 percent of the output reading and was stable after one hour of amplifier operation.

Similarly, the lamp power supply was found to be stabilized after one hour of operation. To simulate field operation and noise pickup, the transmitter and receiver were separated a distance of 9 feet, the light beam properly aligned, and the photocell amplifier output measured while decreasing the input line voltage of the power supply to 87 percent of its initial value. The corresponding change in the amplifier output was less than 0.4 percent. This represented a combined performance of the photocell amplifier and light source stability.

The photocell and amplifier circuit were selected and designed to provide for linearity between illumination and amplifier output. Two linearity checks were performed to determine the true relationship between the photocell illumination intensity and the amplifier output voltage. The first check was performed by utilizing a 15-watt high intensity bulb as a point source of light and causing this light to be focused on the photocell from various known distances and at various levels of intensity. The amplifier output was measured and recorded at each distance and intensity. For a linear illumination-amplifier output to exist, the amplifier output needs to be inversely proportional to the square of the lamp receiver distance during constant light source intensity. This was found to be experimentally true. When the lamp intensity was

varied by varying the voltage to the lamp, the photocell circuit linearity characteristics were determined for very low photocell illumination. By this method the linearity was shown to exist for amplifier output voltages which are greater than 0.0002 volts.

The second photocell amplifier linearity readout check in the laboratory consisted of separating the transmitter and receiver a distance of approximately 12 feet (145 inches) and inserting neutral density filters in the transmitter light beam. The transmitter angle employed in this check was 1.5°, and a receiver angle of view of 0.8°. Six filters having respective neutral densities of 1.0, 0.7, 0.6, 0.4, 0.2 and 0.1 were serially inserted into the light beam and the corresponding output voltage recorded. For each respective neutral density filter the corresponding filter transmittance is given as 10, 20, 25, 40, 63 and 80 percent. The results of plotting known filter transmittance versus reference amplifier output in terms of volts is given in Figure 6.

The angle of view of the receiver was determined by assembling the receiver in a horizontal position at the center of a circle 46 feet in diameter. The distance from the receiver to the circumference was 23 feet and a movement of 4.8 inches along the circumference represented a one degree angle change. This formation was used in determining the angle of view for a small 1.5-inch diameter high intensity light source which was positioned on the 23-foot arc and focused to the receiver. The maximum photocell output was noted and the light source was moved in both directions along the arc until a minimum photocell output was recorded. In the first receiver design, a movement of 7.2 inches of the source either side of the zero angle was required to produce the minimum output reading. This corresponded to a total movement of 14.4 inches or an angle of view of 3 degrees. When this same procedure was employed for the receiver after it was redesigned to reduce the angle of view, it was found that total movement of 3.8 inches caused the receiver to drop to the minimum output value. This showed that the angle of view was then 0.8 degrees.

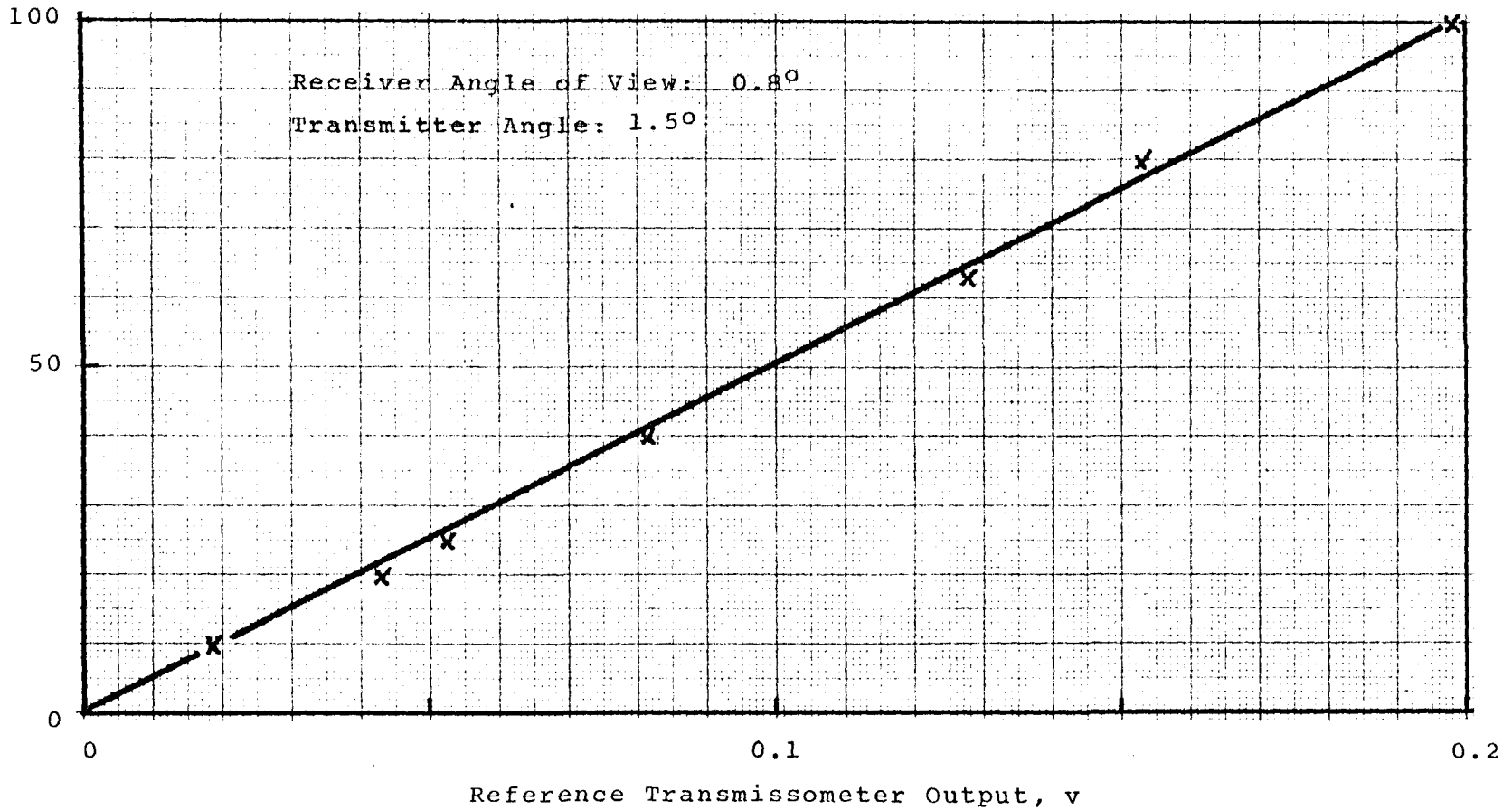

Figure 6. Linearity of the Reference Transmissometer Readout as Determined Using Neutral Density Light Filters.

Prior to installation on the stack, the reference transmissometer was assembled and aligned in the laboratory with an optical path length of 145 inches to obtain a clean air calibration of the entire assembly. This calibration was performed in the laboratory after sunset to obtain dark room conditions. The transmissometer operating characteristics determined for the 3 degree receiver angle were found to be the following during this final laboratory calibration:

1) The collimated transmitter light beam focused on the receiver was 2.5 inches in diameter at the receiver.

2) Operational stability was found to be excellent over a line input voltage variation from 107 to 116 volts. At 104 volt input, the lamp voltage decreases to 6.45 volts from the nominal 6.5 volt value. The resultant decrease in lamp intensity and possible degradation in photocell amplifier circuit at this lower input voltage caused a decrease in photocell output voltage of 0.007 volts or 1.8 percent of nominal value. Increasing the line voltage to 125 volts caused the photocell output for the same controlled lamp voltage to increase by 0.003 volts or 0.8 percent of nominal value. The results of this stability check with regard to line voltage change is shown in Table 1.

3) The reference transmissometer startup and stabilizing period is ten to fifteen minutes. The lamp voltage and photocell output readings recorded during the period of time from applying a constant 116 volt input until stable readings are recorded is shown in Table 2.

Table 1. Stability of Reference Transmissometer With Varying Line Voltages.

Input (volts)	Lamp (volts)	Electrometer Reading (volts)
104	6.45	0.388
107	6.5	0.395
116	6.5	0.395
125	6.5	0.398

Table 2. Stability of Reference Transmissometer During Startup.

Time from Start (min)	Lamp* (volts)	Electrometer Reading (volts)
0	6.3	0.382
5	6.4	0.390
10	6.5	0.395
15	6.5	0.395

*Line voltage constant to 115 volts

Transmissometer performance characteristics were also established for the 0.8° receiver angle and with the exception that the stable (nominal clean air) photocell amplifier output voltage decreased to 0.195 volts, the stability remained the same as for the 3° receiver angle. Nearly identical percent changes in output were found for variations in line voltage in this case.

Experimental Transmissometer

Laboratory evaluations of the experimental transmissometer were performed to determine system stability, angle of transmittance, angle of view, dark current photocell output, and to calibrate the output and determine the accuracy of the instrument.

A lamp power supply voltage of 8.0 volts is the desired operational value and this voltage remains constant with a line input voltage to the power supply over a range of 103 to 130 volts. Over the same range of voltages, the amplifier output signal is constant for each fixed angle of receiver and transmitter. This range of stability was established by repeatedly measuring the lamp voltage and recording the amplifier output for various incremental settings of the power supply input voltage.

The various transmitter light beam angles are achieved by adjusting the light source to a fixed distance from the condenser lens. The light source is mounted in a light tube which slides internal to the aluminum cylindrical housing containing the condenser lens. Therefore, it was

necessary to determine in the laboratory the position of the light tube with respect to the lens. Once the respective distance and position was established for each desired light beam angle, the outer surface of the light tube was scribed and labeled. Establishment of the light tube for each light beam angle (10° increments) was achieved in the laboratory by placing the transmitter a fixed distance from a plain dark wall and focusing the positioned light source/condenser beam onto the wall. The resultant light beam diameter on the wall was measured and, knowing the distance from the source to the wall, the sine/cosine relationships were employed to determine the resultant transmitter light beam angle. In actuality, the required light beam diameters for each desired light beam angle were marked on the wall and the light tube adjusted until that diameter beam was obtained. By this method the transmitter was calibrated for zero degree and in ten degree increments up to the maximum beam angle of 100°.

The experimental transmitter viewing angle range was established in the same manner as that described for the reference transmissometer. By this method it was found that the minimum viewing angle of the experimental transmissometer was 2° and the maximum was 120°.

For various viewing angles within this range, the viewing angle adjustment mechanism was calibrated and scaled to provide for 10° incremental changes. Below 5° a special pinhole plate was constructed and needs to replace the iris to achieve the 2° angle of view.

The "dark current" reading of the photocell, preamplifier and amplifier circuitry of the experimental transmissometer was determined by eliminating all light to the photocell and measuring the resultant amplifier output signal. Readings were obtained for all three preamplifier range settings with a Keithley 502 electrometer. The results are shown in Table 3.

Table 3. Dark Current Signal of Experimental Transmissometer Receiver.

Preamplifier Range	Dark Current Reading (volts)
X1	-0.00075±0.00005
X10	-0.0065 ±0.0005
X100	-0.0660 ±0.005

As shown by the table, for all preamplifier ranges the "dark current" phenomena yields a negative voltage signal. These readings are characteristic of most photocells and the value is magnified by the increased preamplification. However, because of its small value it was found to be difficult to eliminate electronically and achieve a true base zero for no illumination. Therefore, for accurate transmittance determinations the zero point offset must be corrected for arithmetically. In use, the measured values for any transmittance are increased by the amount of the absolute "dark current" amplifier reading specific for the amplifier range selected (X1, X10, X100).

The linearity of the photocell amplifier circuitry was determined by the same two(point light source and neutral density filters) techniques as described for the reference transmissometer. For the point light source technique the quantity of light reaching the photocell was varied by changing the distance between source and the receiver. The intensity of light to the receiver follows the inverse square law as given by Equation (6):

$$E = KL^{-2} \qquad (6)$$

where

E = amplifier output, volts

K = constant

L = optical path between source and receiver, feet.

The corollary to Equation (6) with the data obtained for each of the three preamplifier ranges was:

$E = KL^{-2.38}$ for the X1 range over values of E from 0.0014 to 0.028

$E = KL^{-2.19}$ for the X10 range over values of E from 0.018 to 0.28

$E = KL^{-2.19}$ for the X100 range over values of E from 0.031 to 2.8.

The correlation coefficient for each set of linearity measurements were within 0.995 to 0.999. Even though the linearity was not defined at the "dark current" values, it is expected from the experience with the reference transmissometer that acceptable linearity is also achieved at lower levels of illumination.

In the case of the neutral density filter technique to determine photocell and related circuitry linearity, tests were performed for 2° angle of view and for transmitter angles from 0 to 60°. As shown in Figure 7, the linearity is good over the range of transmitter angles from 10° to 60°. At the near 0° transmitter angle the generated data was not of sufficient quality to establish a good linear relationship. The reason for this condition was that the condenser of the light energy created a discoloration with the center and edges of the light beam at this angle of focus and ND filters used appeared to be color-sensitive.

A calibration of the experimental transmissometer was performed to determine the experimental transmitter light intensity at the optical distance for the transmitter and receiver of 145 inches, and for receiver light angles of 2, 4, 5, 6.5, 8.5, and 16°. Additionally, the transmitter light angle was varied over the range of from 0° to 100° in 10 degree increments. The receiver photocell amplifier output corresponding to each transmitter light angle used was measured by a Keithley 502 electrometer with no interference filters inserted in the receiver optical system, and the procedures repeated for 0.436, 0.486, 0.534 and 0.656 micron light interference filters.

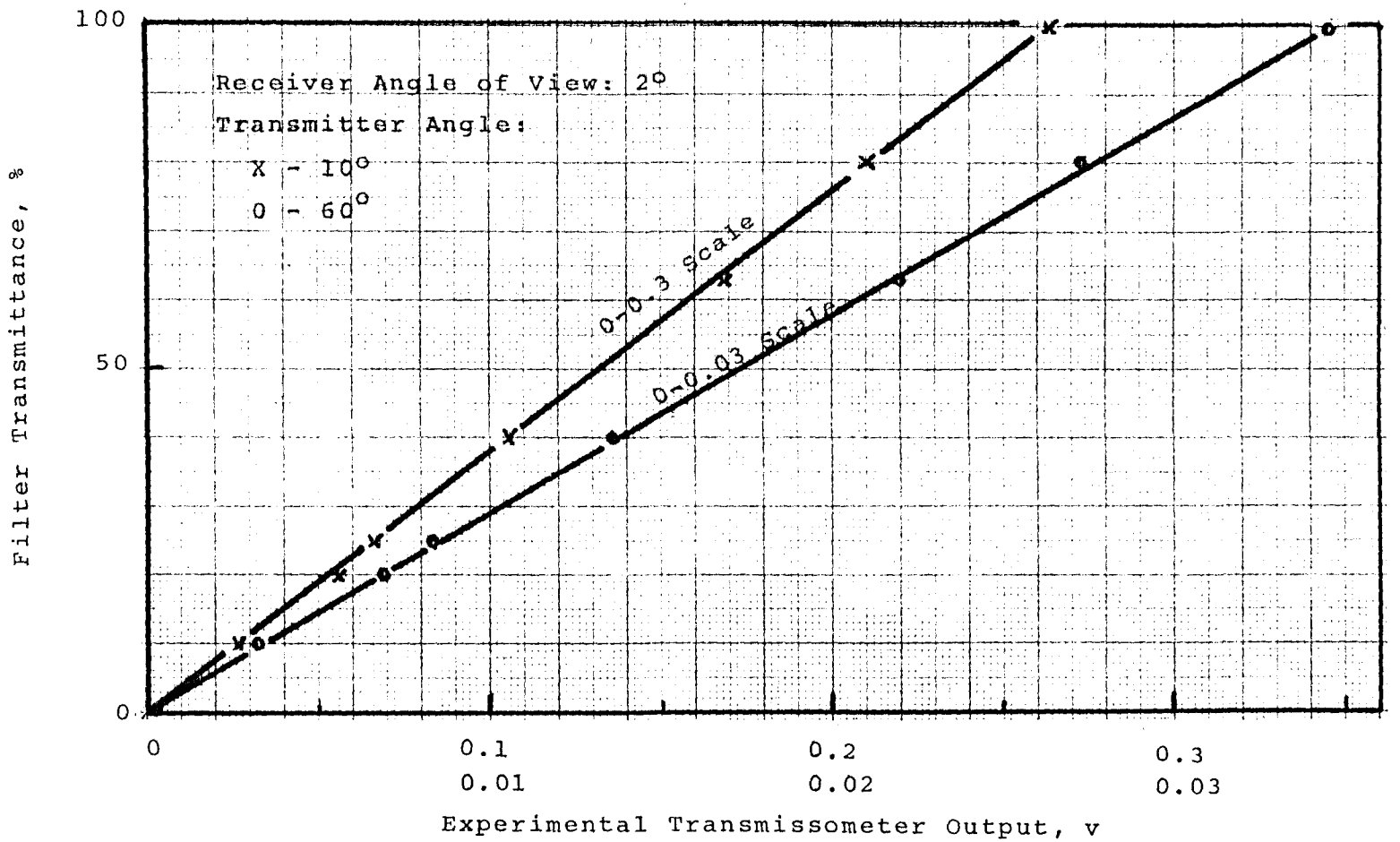

Figure 7. Linearity of the Experimental Transmissometer Readout as Determined Using Neutral Density Light Filters.

The illumination lamp voltage of 8.0 volts was set and used throughout the experiments. A near linear relationship between the amplifier output signal and the transmitter light angle was found, except for the near 0^{o} transmitter angle. For any given receiver angle this relationship can be expressed by Equation (7):

$$E = K \times \varepsilon^{b} \qquad (7)$$

where

E = amplifier output, volts

K = constant

ε = transmitter light angle, degrees

b = exponent

The results of the experimental transmissometer output calibration are tabulated and presented in Appendix A of this report. The data are presented for transmitter angles from 0 to 60 degrees and receiver angles 2, 4 and 6.5 degrees. For larger receiver angles, the photocell output signal for 6.5 degrees can be used because it was found that the output is no longer dependent on the receiver angle magnitude above this value.

Using the calibration data the accuracy of in-stack transmittance determination can be calculated. The accuracy is generally decreasing with increasing transmitter light beam angle because the light intensity as seen by the photocell also decreases. This same tendency is also seen when interference filters are used in the receiver.

Table 4 contains the calculated accuracy for a given transmittance when the transmissometer is operated at 100 degrees transmitter angle, 4 degrees receiver angle and with various interference filters in position.

Table 4. Calculated Accuracy of Transmittance Measurements.

Illumination of Filter	Transmittance* (%)	Accuracy as Percent of Transmittance	Accuracy of Transmittance (%)
White Light	0.8	±10	±0.08
0.436 μm	30	±15	±4.5
0.486 μm	10	±5	±0.5
0.534 μm	5	±2.5	±0.13
0.656 μm	5	±2.5	±0.13

*Measured with 100° transmittance angle, 4° receiver angle.

SECTION VII

FIELD TESTS

Field Facilities and Conditions

The number eleven pulverized coal-burning 100 MW boiler and associated stack located at the Northern States Power Company Highbridge Plant in St. Paul, Minnesota was selected and approved as the test site. Tests performed in January of 1970 on this boiler revealed the following data as measured downstream of the electrostatic precipitator: gas flow of 388,000 scfm; stack gas temperature about 200°F; average dust concentration 0.095 gms/ft^3; precipitator collection efficiency approximately 93 percent.

As shown schematically in Figure 8, this stack is of cylindrical steel construction approximately 12 feet in diameter and 292 feet tall. The measured internal diameter of the stack is 145 inches and this dimension is also the effective light path length with the transmissometers located in position. The stack protrudes through the boiler room roof which is 110 feet above the ground. Within the boiler room, the boiler gases pass to a split flow electrostatic precipitator from which two separate gas streams exit and enter the stack just above the roof line through two diametrically opposite but identical ducting systems. The experimental transmissometer was positioned on the stack 50 feet above the roof. The reference transmissometer was located 12 feet higher up. The 12-foot spacing between transmissometers was determined to be sufficient to prevent any interference between transmitters during simultaneous operation.

Both transmitters and receivers were mounted on the stack wall using directionally adjustable ports and special brackets welded to the stack wall supporting the instruments and locking them in the position desired. Special attention was given to locating the optical system of the experimental transmitter and receiver close to the gas stream flow boundaries to permit the evaluation of as large transmitting light angles as possible.

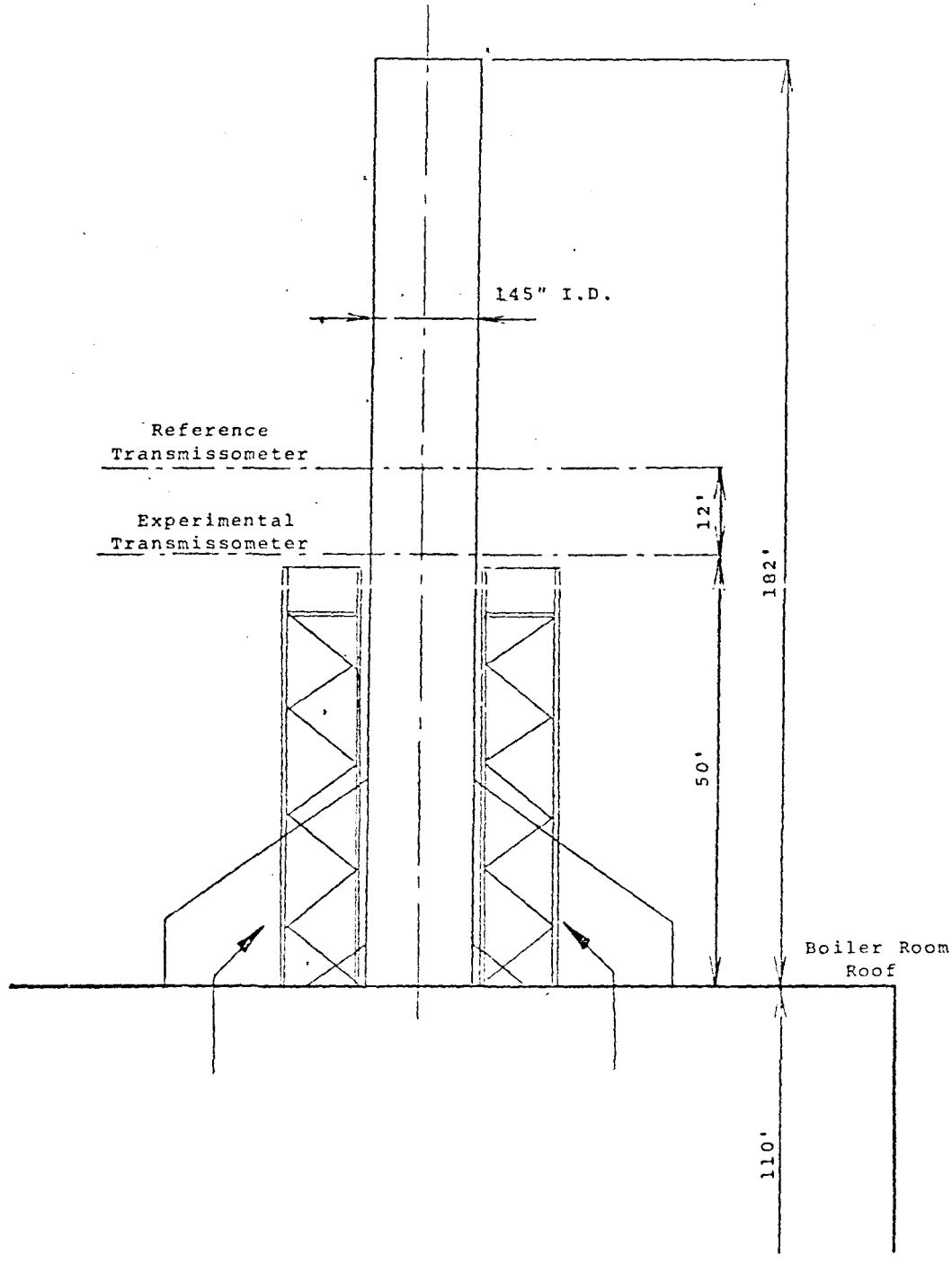

Figure 8. Experimental Stack Dimensions and Port Locations.

Two separate scaffoldings attached to the stack provided a base for the transmitter and receiver operators. The transmissometers were electrically connected with sufficient lengths of shielded cabling to the readout instruments located in a shelter on the boiler room roof.

During the field evaluation the boiler was energized with a mixture of approximately 10 percent Western Montana powdered coal and 90 percent Illinois coal. Boiler operation was steady during the periods of testing, but electrostatic precipitator rapping, performed at one-minute intervals for about 15 seconds, caused some fluctuations in the actual stack gas transmittance, as seen in Figures 10 and 11. The plant supervisor and engineer allowed the investigators to vary the electrostatic precipitator's high voltage power supply to obtain plume opacities within limits of 40 to 90 percent. This was helpful in obtaining data for a wide range of the plume opacities, but evaluation and interpretation of results became more difficult. This difficulty may have arisen from a change in the particle collection efficiency of the precipitator for various-sized particles, as the voltage was varied, causing variations in the effluent particle size distribution. Having no quantitative information about particle size changes, no consideration could be given to the changed optical properties of particulates in relation to the plume transmittance.

The location which provided the best view of the plume and permitted optimum opportunity for obtaining contrasting target plume opacity measurements was a river bank located about 700 feet southeast of stack number eleven. From this location the plume, as it exited from the stack, was readily visible. A concrete stack under construction at the time extended above and to the left of stack number eleven and served as the contrasting target for the proper plume opacity determinations. A photograph of the two stacks as taken from the plume viewing location is shown in Figure 9.

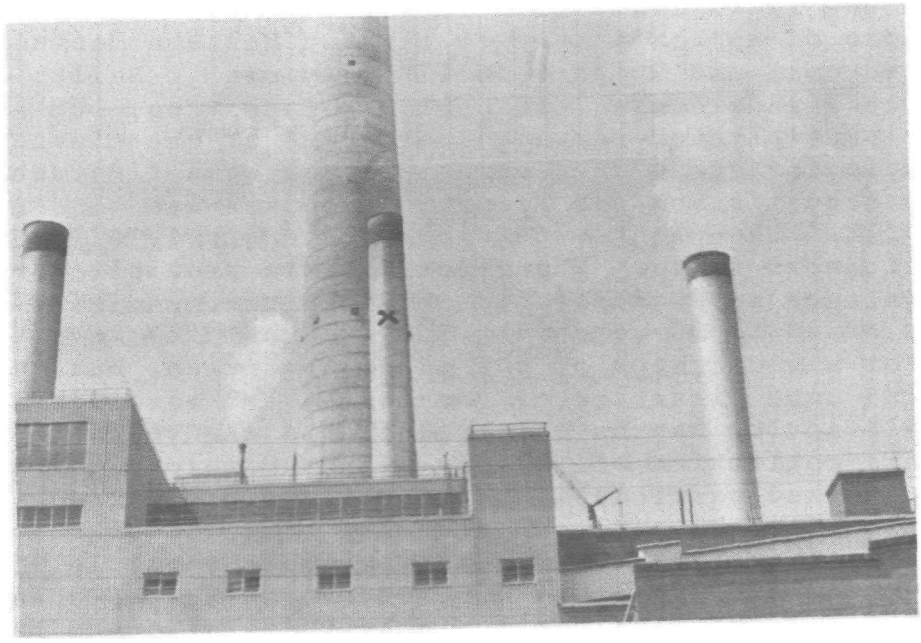

Figure 9. Experimental Steel Stack* Viewed Against the Concrete Stack Used as the Contrasting Target for the Telephotometer Measurement of Plume Transmittance.

Field Optical Alignment of Instruments

Each time the transmissometer was installed on the stack, the following procedure was followed to assure proper alignment of the instruments:

1) The transmitter light beam angle was set to the minimum value to obtain a collimated light beam.

2) The covers over the closed mounting ports were opened and the transmitter was positioned in the holder.

3) The transmitter was energized and aligned so that the light beam was observed through the receiver port opening. Alignment is achieved by the observer on the receiver port side viewing the beam and directing the individual controlling the transmitter to perform the necessary adjustment until the maximum light intensity is visually realized.

4) The receiver is then positioned in its holder and slowly adjusted up-down and left-right until the maximum photocell output signal is established.

5) When proper alignment is achieved, the transmitter and receiver are physically locked in position.

During the course of the field tests, each transmissometer was removed and re-installed on the stack several times. It was found that near identical alignment and reproducibility in results could be achieved very rapidly by following the above-noted procedure. The need for repeated installation was necessary because the demand for electrical energy by the customers of Northern States Power Company would not permit a shut-down of the boiler for periodic clean air baseline photocell measurements. Furthermore, rigid routine lens and other component inspection schedules were maintained to eliminate the possibility of obtaining erroneous information. The air flushing system of the transmissometers performed properly for all components except the experimental transmitter, where it was necessary

to essentially expose the condenser lens to the flue gas particles in order to obtain maximum transmitter angles. Due to the close proximity of lens and contaminated particles, this transmitter was removed during testing activities every 60 minutes for particulate cleaning if needed and examination of the lens.

Field Data Procurement

With the transmissometers properly aligned and operating, the photocell readout from each transmissometer was recorded on a Bausch & Lomb VOM-5 strip chart recorder. Examples of the resultant chart recordings obtained are shown in Figures 10 and 11. The reference transmissometer output recording was readily related to the plume opacity and used to determine true in-stack transmittance. The experimental transmissometer readings were related to the reference transmittance to evaluate the effect of the various modes of operation.

Chart recordings of Figures 10 and 11 show only the period of opacity fluctuations during the time electrostatic precipitator rapping was occurring. The elapsed time is approximately 15 to 20 seconds, and each of these periods were followed by relatively steady opacity period of about 40 to 45 seconds duration.

For most experiments the sequence of the data taking was to scan the transmitter light beam angles from 0 to 60 degrees for a constant angle of view with and without interference light filters in the receiver. The angles of view of the experimental receiver that were tested were: 2, 3, 4, 5, 6.5, 8.5, 10, 16, 20, 30, 40, 50 and 60 degrees. Transmitter angles of near 0, 10, 20, 40 and 60 degrees were scanned.

Weather conditions permitting, telephotometer measurements of the out-of-stack transmittance were taken using the technique of contrasting targets.

During some of the tests, samples were collected from the stack through the experimental transmissometer port in order to obtain some information on the size distribution of the effluent particulates. An isokinetic probe, incorporating a filter holder containing a glass fiber absolute filter

Run:	10b - 3/22/72
Transmitter:	10°
Receiver:	40°
Filter:	None

EXPERIMENTAL TRANSMISSOMETER

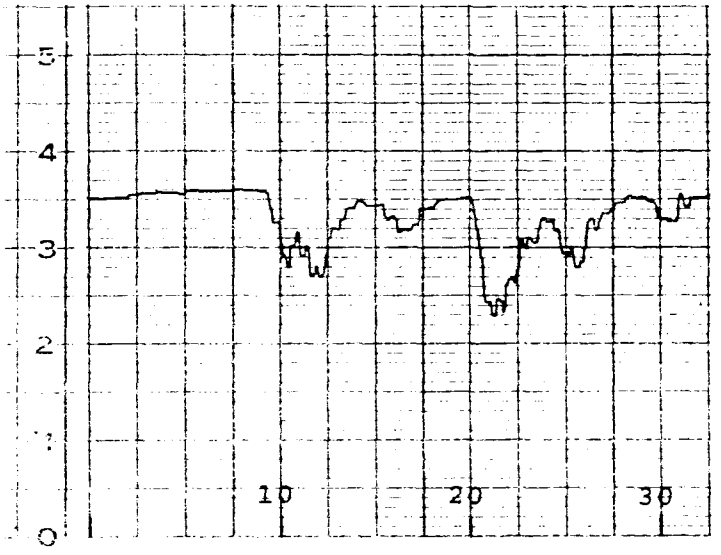

Time, seconds

REFERENCE TRANSMISSOMETER

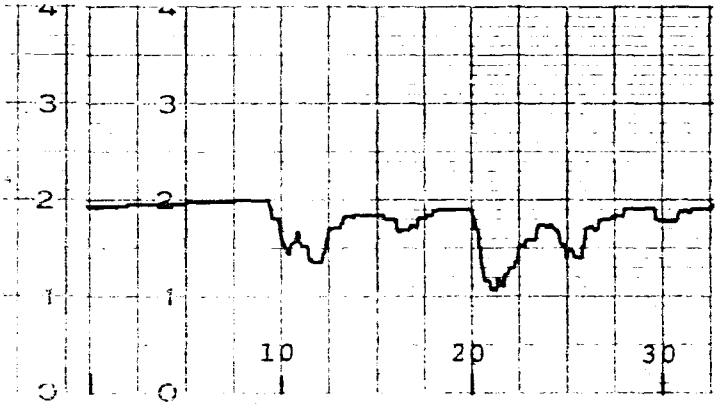

Time, seconds

Figure 10. Example of the Experimental Data Recorded in the Field Test.

Run: 5a - 3/22/72
Transmitter: 0°
Receiver: 3°
Filter: 0.656μm

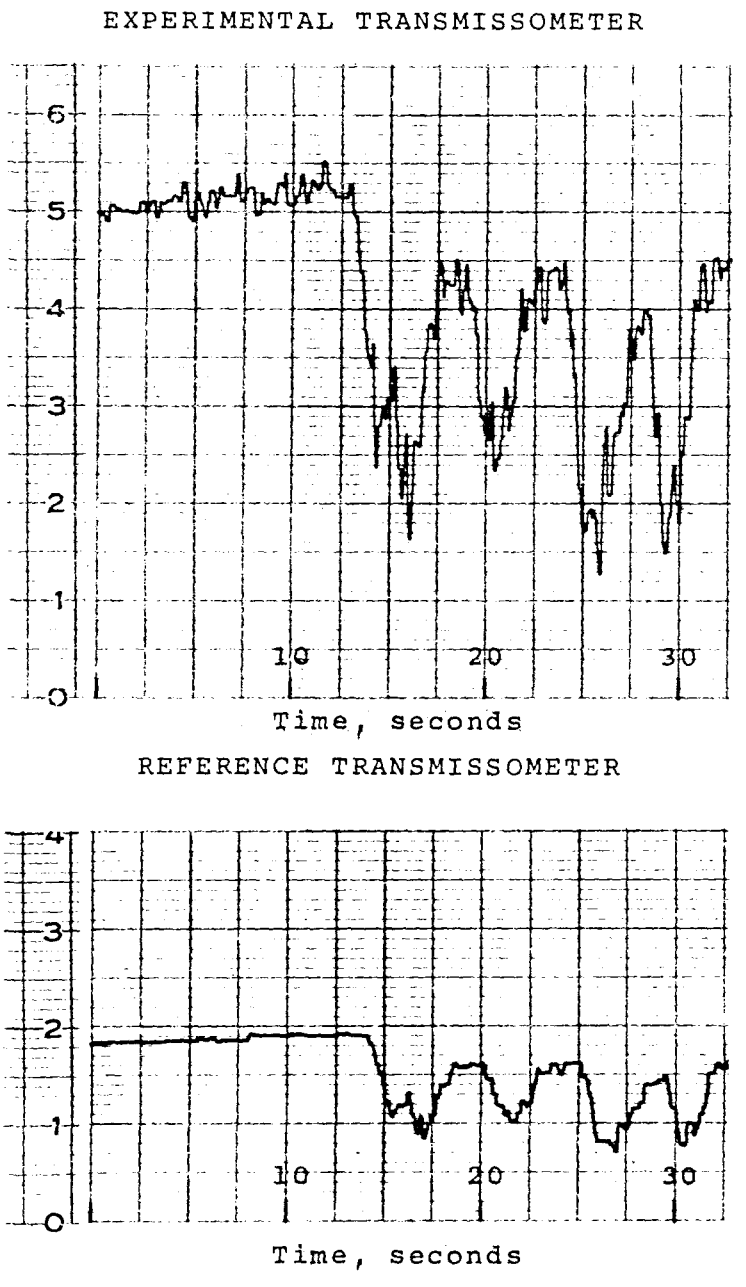

Figure 11. Example of the Experimental Data Recorded in the Field Test.

(Gelman Type E) was located in the gas flow, 4 feet from the stack wall. The probe was allowed to equilibrate to the stack temperature and a sample was drawn through the filter where the particulate collection occurred. The dust collected was evaluated for particle size using optical and electron microscopy.

Evaluation of Field Transmittance Data

The basic parameters measured and recorded in the field for further evaluation were the reference and experimental transmissometer output signals and the telephotometer readings. The reference and experimental transmissometer measurements are used to calculate the in-stack transmittance and to describe the effects of operating the experimental transmissometer with defined operational parameters (i.e., transmitter and viewing angles). The reference in-stack transmittance is calculated by use of Equation (8):

$$T_R = \frac{E_{RT}}{E_{RTO}} \qquad (8)$$

where

T_R = calculated in-stack reference transmittance, dimensionless

E_{RT} = measured in-stack reference transmissometer photocell output signal, volts

E_{RTO} = reference transmissometer photocell output signal for 100 percent transmittance. Determined in the laboratory for a defined optical path of 145 inches and for the transmitter angle of 1.5°. For 3° receiver angle, E_{RTO} = +0.240 volts; for 0.8° receiver angle the E_{RTO} value is +0.195 volts.

The experimental in-stack transmittance is calculated by means of Equation (9):

$$T_E = \frac{E_{ET}}{E_{ETO}} \qquad (9)$$

where

T_E = experimental in-stack transmittance, dimensionless

E_{ET} = "dark current" adjusted photocell output, volts

E_{ETO} = "dark current" adjusted calibration photocell output for laboratory determined 100 percent transmittance at a given transmissometer setting, volts

E_{ET} was determined by adding the established "dark current" reading to the measured value. The "dark current" value to be added is dependent on the preamplifier scale used to obtain the measurements. The proper values as determined in the laboratory are given in Appendix A.

Different E_{ETO} values were developed in the laboratory for each defined receiver and transmitter angle listed and for each interference filter employed. The established values are given in Tables 1 through 3 of Appendix A.

In spite of relatively good short term flue gas stability, changes in transmittance were detected by the reference transmissometer during prolonged periods of data taking. Therefore, in order to compare data from one readout period to the next, the experimental transmittance data was normalized by applying the proper values in Equation (10):

$$T_{E_{norm}} = \frac{T_E}{T_R} \times \overline{T}_R = \frac{1}{T} \times \overline{T}_R \qquad (10)$$

where

$T_{E_{norm}}$ = normalized experimental transmittance, %

T_E = measured experimental transmittance, %

T_R = reference transmittance corresponding to T_E %

$\bar{T}_R$ = average reference transmittance for the defined array of measured experimental transmittance values being normalized

$T = T_R/T_E$ relative in-stack transmittance.

By this method of normalization the normalized experimental transmittance values are based on an average reference transmittance for the defined array of measured experimental transmittance values, and all values so normalized can be compositely compared and analyzed.

The plume transmittance was calculated from Equation (4).

SECTION VIII

RESULTS AND DISCUSSION

Plume and Reference In-Stack Transmittance Relationship

The average values of the reference in-stack and telephotometer plume transmittance are presented in Table 5 and plotted in Figure 12. These results are for the reference transmissometer operated with a 1.5° transmitter angle and a 3° angle of view. As seen from results in Figure 12, a plot of the experimental data provides a line which has a slope just above unity. With perfect agreement, the data should have fallen on the unit slope line. It can be seen by the data points that for transmittance close to 100 percent this is indeed realized. For lower transmittances, the measured in-stack transmittance was slightly higher. This could be due to the detection of scattered light by the 3° angle of view of the in-stack transmissometer used in these experiments.

Table 5. Data on the Plume Transmittance vs. In-Stack Transmittance Correlation.

NOTE: Plume transmittance measured by Spectra SB 1/2 Brightness Spot Meter by means of contrasting targets technique; angle of view 0.5°. In-stack transmittance measured at 1.5° transmitter angle and about 3° of the angle of view.

Out-of-Stack Transmittance (%)	In-Stack Transmittance (%)
84	87
80	81
78	76
70	74
69	68
53	56
48	49
47	53
41	46
36	38

Linear regression of the data: Slope = 1.049; y intercept = -5.316; correlation coefficient = 0.99.

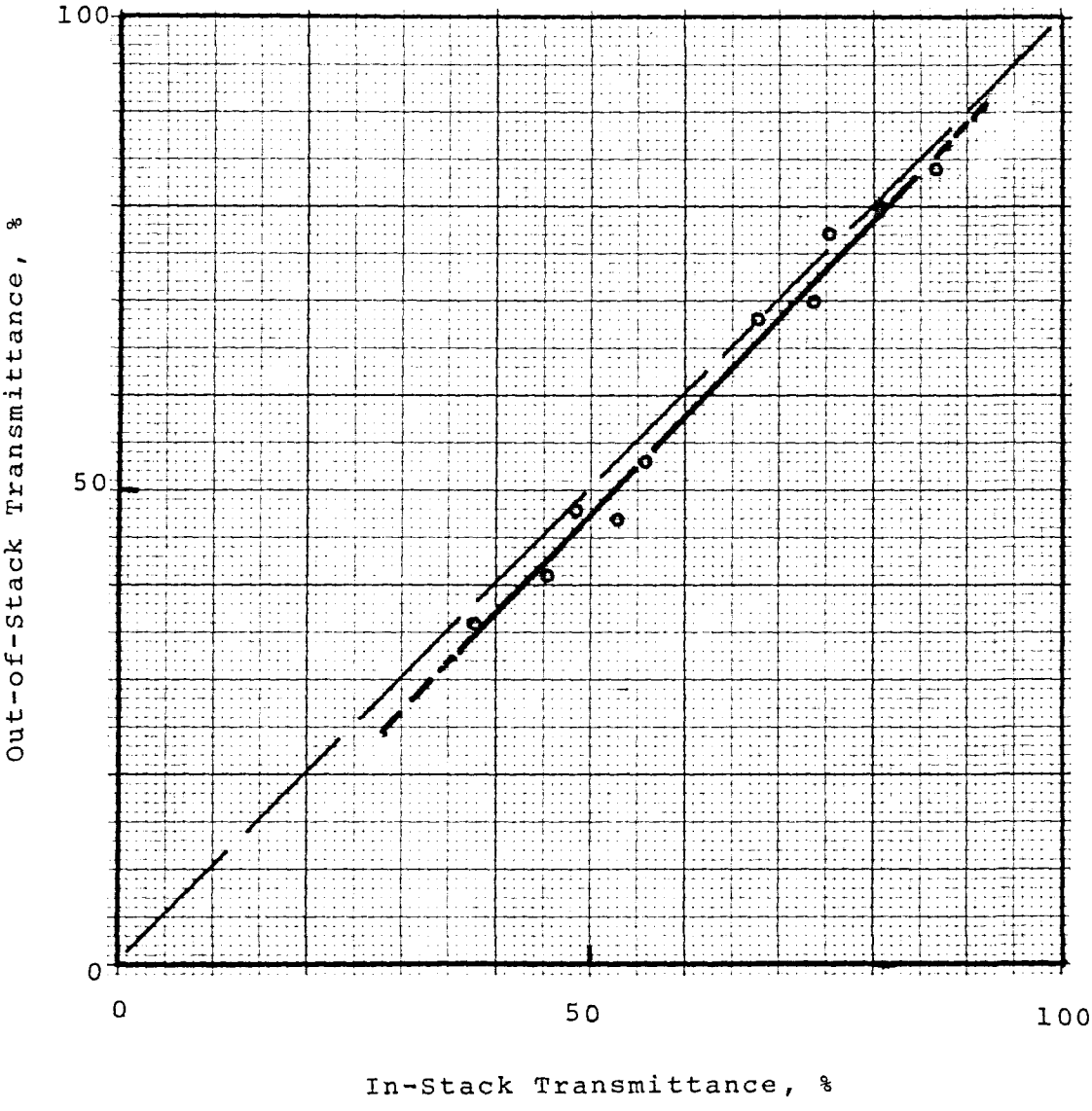

Figure 12. Transmittance Measurements by 3° Angle of View and 1.5° Illumination Angle Transmissometer Inside Stack and 0.5° Angle of View Telephotometer Outside Stack.

In-Stack Transmittance vs. Experimental Transmitter and Receiver Angle Characteristics

As previously discussed, all of the experimental transmittance data were normalized prior to studying the effect of the various transmitter and receiver angles.

A plot of the normalized in-stack experimental transittance versus the operational receiver angles is shown in Figure 13 for various transmitter angles. The line describing the transmittance for a near 0° transmitter angle is shown as a dashed line to indicate that it is based on widely scattered experimental data due to the effect of light beam discoloration caused by the condenser lens at this small angle. However, the data clearly indicated the same trend as shown for the larger transmitter angles.

The data shown in this plot demonstrates that the measured transmittance is strongly dependent on the receiving and transmitting angles. The contribution of light scattered to the receiver from particles inside and outside the field of the receiver view is given as the reason the experimental transmittance is always higher than the corresponding reference in-stack transmittance.

From Figure 13 the error due to any combination of transmitter and receiver angle can be determined. For example, the error is about 9 percent for a receiver angle of 5° and a 10° transmitter angle.

Data similar to that presented in Figure 13 but for lower values of average in-stack reference transmittance were reviewed during the course of the study and similar type curves were generated. For lower in-stack transmittance the difference between reference transmittance and experimental transmittance was greater for all combinations of receiver and transmitter angles investigated. This phenomena may be due to an increase in size of particles in the stack at the time of the lower transmittance measurements. The lower transmittance in the stack was created by decreasing the voltage in the electrostatic precipitator and, consequently, it is very likely that a difference size distribution of particles would penetrate the precipitator. A changed particle size distribution flowing through the light beam would reflect a change in the relative amount of light scattered to the receiver. Ensor and Pilat[3] have shown theoretically the effect of particle size and transmissometer receiving angles on transmissometer measurements.

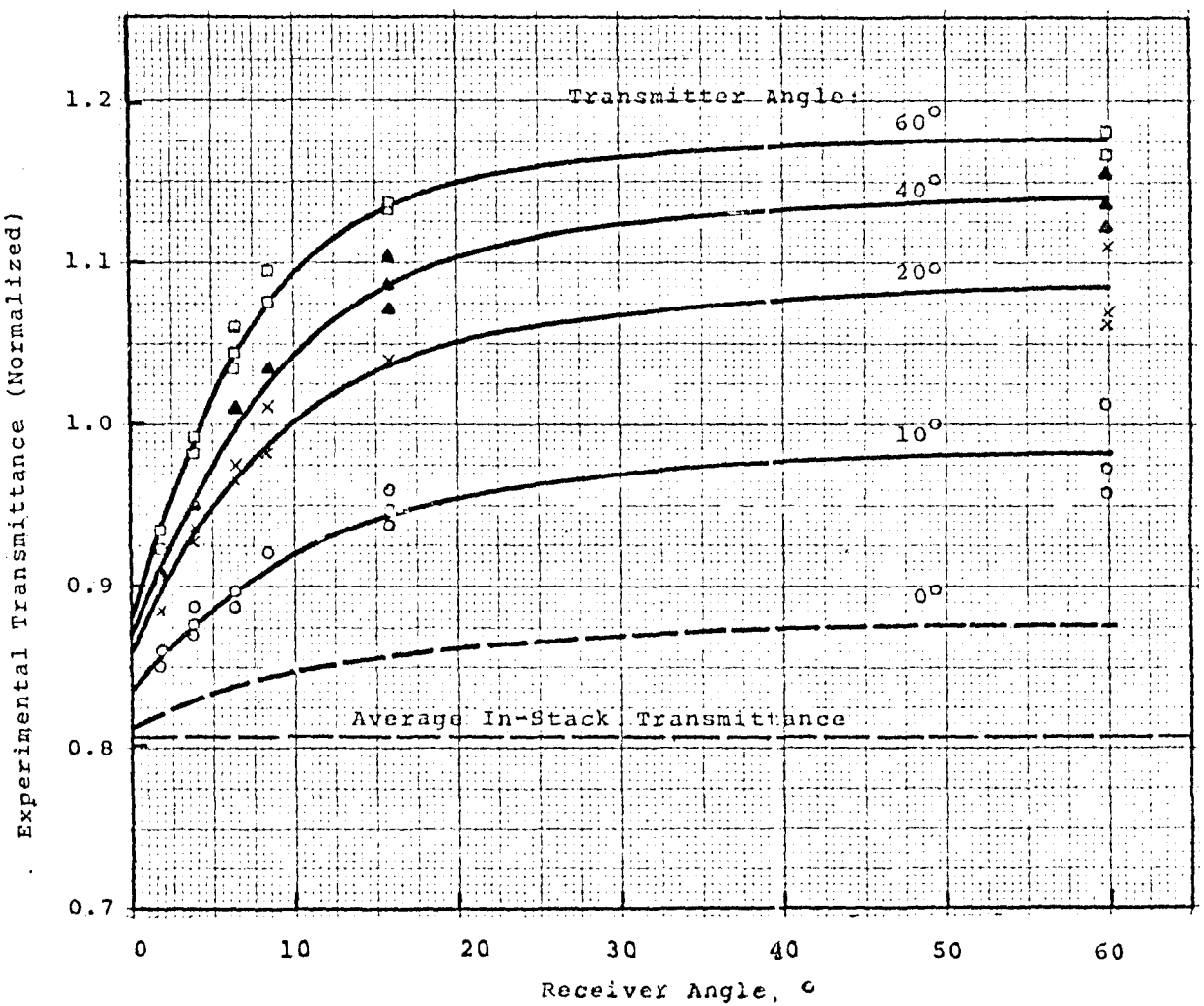

Range of In-Stack Reference Transmittance: 0.607-0.880

Average In-Stack Reference Transmittance: 0.807

Interference Filter: None

Run: 1, 6, 7, 8, 9, 12 of 4/19/72

Reference Transmissometer Viewing Angle: 0.8°

Illumination Angle: 1.5°

Experimental Transmittance Normalized to 0.807 In-Stack Reference Transmittance

Figure 13. In-Stack Experimental Transmittance Detected at Various Transmitter and Receiver Angles of the Experimental Transmissometer Normalized for True Reference In-Stack Transmittance of 0.807.

These results show that both the receiver and transmitter angles of a transmissometer should be as small as practical to restrict the detection of scattered light and the associated error.

In-Stack Transmittance-Wavelength Characteristics

Tests with four different light interference filters, namely 0.436, 0.486, 0.579, and 0.656 micron wavelength, inserted in the light path before the experimental receiver photocell were performed to define the measured transmittance as a function of wavelength. The results of this group of experiments are seen in Figure 14 where the normalized experimental transmittance is plotted versus transmitter angle for all four filters evaluated. These plots show the dependence of the in-stack transmittance on wavelength. The 0.656 micron interference filter yields the lowest in-stack transmittance. The transmittance increases with each incremental decrease in wavelength evaluated. This result would indicate that spectral absorption effects were present and/or the particulates were larger than about one micron and sufficiently monodisperse to observe oscillation of extinction efficiency with wavelength. Microscopic analyses of particulate samples indicated the number mean diameter of around 1.4 micron and geometric standard deviation of around 1.6.

The trend for the difference between the measured experimental transmittance and reference or plume transmittance to become greater for generally decreasing transmittance was also seen in this set of data. Also, the value of the experimental measured transmittance is more dependent on the magnitude of the receiver angle when filters are employed. This phenomena results in generally larger experimental transmittance values to be measured with relation to the reference transmittance, and may be again caused by differences in the effluent particle size distribution influencing the light scattering characteristics.

Secondly, the rate of change in the difference between experimental and reference transmittance is greater for increasing receiver and transmitter angles when filters are utilized. This phenomena may be caused by different light scattering characteristics of the effluent, due to larger fly ash particles present during the "interference filters" experiments.

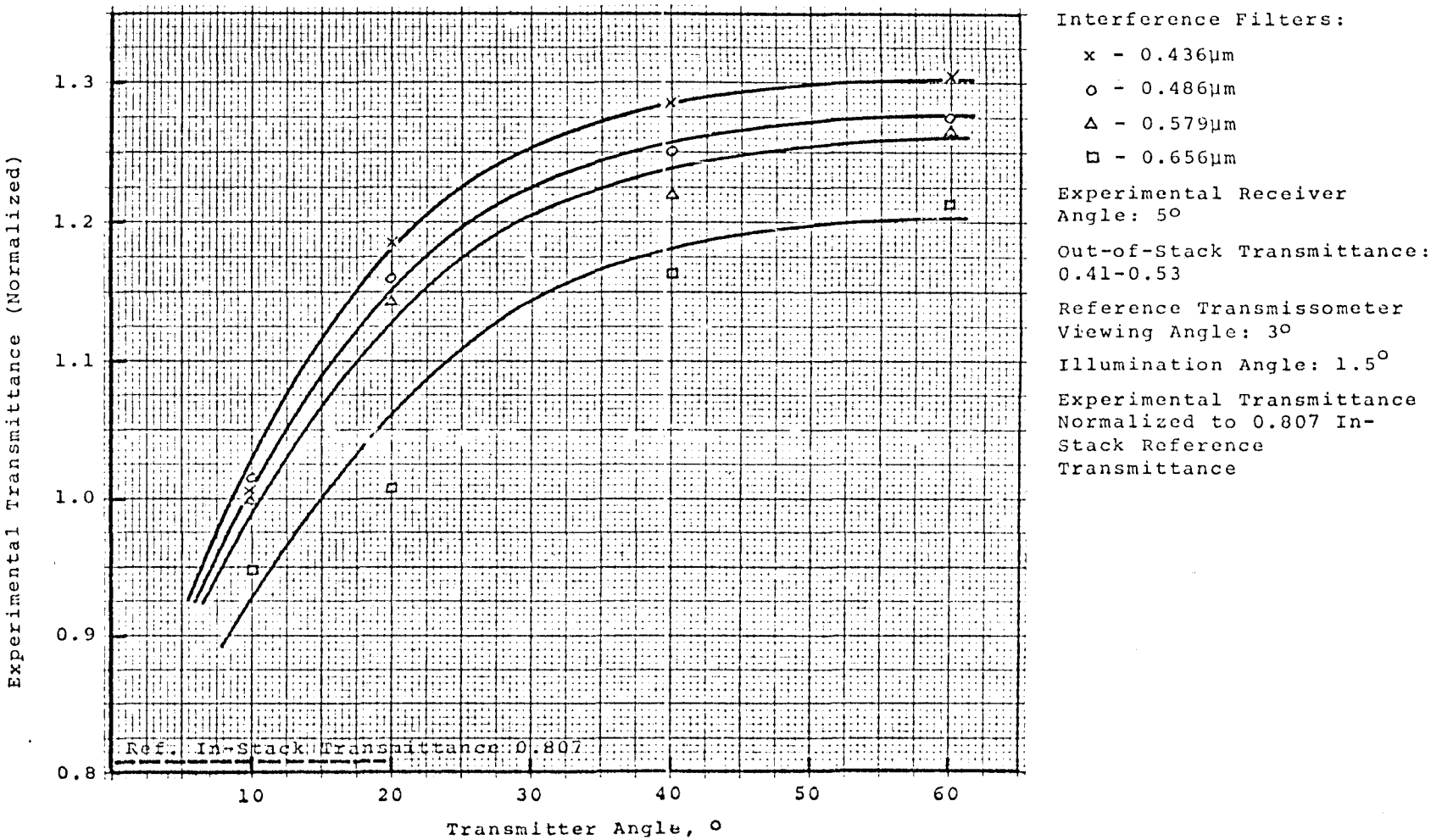

Figure 14. Summary of Interference Filter Tests. Relationship of the Experimental In-Stack Transmittance and Transmitter Angle for Four Interference Light Filters at 5° Receiver Angle.

Evaluation of the transmittance data shows that the closest agreement between in-stack and plume transmittance measurements are achieved when either white light or an interference filter between 0.486 and 0.579 micron is used.

SECTION IX

ACKNOWLEDGEMENTS

The work described in this report was performed by Environmental Research Corporation (ERC), St. Paul, Minnesota, under EPA Contract No. 68-02-0309 by a team consisting of Dr. Carl M. Peterson, Dr. M. Tomaides, Ben Wahi, Keith Rust, Bob McKimmy, Len Graf and Roger Johnson.

The contract was administered under the direction of the U. S. Environmental Protection Agency (EPA), with Mr. William D. Conner as Project Officer. The authors wish to thank Mr. Conner for his valuable contributions and guidance.

Also, they wish to express their appreciation to all workers of Northern States Power Company for their kind assistance throughout the field experiments; namely, to Mr. Dave Williams, Patrick Gordon and Tom Anderson.

SECTION X

REFERENCES

1. Hodkinson, J.R., "The Optical Measurement of Aerosols", In: Aerosol Science. Edited by C.R. Davies, Chapter X, p. 287, Academic Press, New York, New York 1966.

2. Conner, W.D., and J.R. Hodkinson (1966), "Observations on the Optical Properties and Visual Effects of Smoke Plumes", Environmental Health Service, U.S. Govt. Printing Office, PHS Publication No.999-AP-30.

3. Ensor, D.S. and M.J. Pilat (1971), "The Effect of Particle Size Distribution on Light Transmittance Measurement", Am. Ind. Hyg. Assoc. J., 32, 287-292.

SECTION XI

APPENDICES

APPENDIX A

EXPERIMENTAL DATA

Results of Experimental Transmissometer Calibration

Results of laboratory experimental transmissometer calibration are presented. When calibrating the instrument in the laboratory, the transmitter and receiver were optically aligned and firmly attached in that position on two separate heavy laboratory benches, 145 inches apart. The output of the receiver photocell signal amplifier was monitored with a high input impedance Keithley 602 Electrometer and by a Bausch & Lomb strip chart recorder. For constant setting of the receiver angle of 2, 3, 4, 5 and 6.5 degrees, the transmitter angle was adjusted from 0 to 100 degrees, and for each angle, the amplifier output measured. This procedure was repeated for four different interference light filters after taking data for the transmissometer operation without any light filter in the line. The data taken were corrected for "dark current" photocell operation that was determined by closing the receiver inlet and reading the amplifier output signal under this condition. The "dark current" was -0.00075 volt for "low" preamplifier setting on the receiver panel, and -0.00650 volt for "medium" switch position.

To correct the amplifier output readings, the following equation was used:

$$E_{COR} = \pm E_M - (E_{D.C.})$$

where

E_{COR} = corrected output

E_M = amplifier output reading(was negative for low photocell illumination), volt

$E_{D.C.}$ = "dark current" amplifier output:
-0.00075 volt "low" preamplifier
-0.00650 volt "medium" preamplifier

The resulting corrected photocell amplifier outputs are tabulated for no interference filter in Table A-1;for 0.436 micron filter in Table A-2; and 0.656 micron filter in Table A-3; and the data can readily be used for experimental data evaluation or for future transmissometer useage when the optical path length is 145 inches.

Field Determination of "Dark Current"

With the instruments optically aligned and attached to the stack, the "dark current" amplifier output was determined by closing the receiver inlet. Because this value depends on the photocell temperature, this procedure was repeated every hour during data taking process. This detected "dark current" amplifier output was used to correct the outputs determined for various experimental transmissometer operational conditions. The procedure used in correcting measured data for "dark current" conditions was identical to that described in the transmissometer calibration section.

In-Stack Transmittance-Wavelength Characteristics

Tests with four different light interference filters, namely 0.436, 0.486, 0.579 and 0.656 micron wavelength, inserted in the light path before the experimental receiver photocell were performed to define the measured transmittance as a function of wavelength illumination or detection.

The results of this group of experiments are plotted in Figures A-1, A-2, A-3 and A-4. In these figures the relative transmittance defined in Equation (10) is plotted against the receiver angle as a function of the various transmitter angles. As previously defined, the larger the relative transmittance number, the lower the measured experimental transmittance or normalized values. It must be noted that the true in-stack transmittance used in calculating the relative transmittance was measured with the 3° receiver angle reference transmissometer. Based on the results described in Section VIII, all transmittance values in Figures A-1, A-2, A-3 and A-4 would have been about 5 percent lower if the 0.8 degree receiver angle reference transmitter had been used. Such a correction would be necessary if interference filters results and no interference filter results are to be compared.

Table A-1. Results of Experimental Transmissometer Calibration.

Transmitter Angle (degrees)	Receiver Angle (degrees)	Interference Filter (μm)	Photocell* Amplifier Output (Corrected) (v)
0	2.0	None	2.82075
10	"	"	0.26375
20	"	"	0.09725
30	"	"	0.06055
40	"	"	0.04825
50	"	"	0.04025
60	"	"	0.03455
0	4.0	None	3.35075
10	"	"	0.32075
20	"	"	0.12475
40	"	"	0.06375
60	"	"	0.04475
0	6.5	None	3.38075
10	"	"	0.33575
20	"	"	0.13275
40	"	"	0.06625
60	"	"	0.04675

*Data are valid for "Low" pre-amplifier setting on the experimental receiver cover. For "Medium" setting, multiply values by 10. Setting "High" is not recommended.

Data corrected for the following "dark current" amplifier outputs:

"Low" pre-amplifier setting = -0.00075 volt

"Medium" pre-amplifier setting = -0.00650 volt

Table A-2. Results of Experimental Transmissometer Calibration.

Transmitter Angle (degrees)	Receiver Angle (degrees)	Interference Filter (μm)	Photocell* Amplifier Output (Corrected) (v)
0	2.0	0.436	0.08975
10	"	"	0.00240
20	"	"	0.00075
30	"	"	0.00043
40	"	"	0.00032
50	"	"	0.00026
60	"	"	0.00022
0	4.0	0.436	0.11275
10	"	"	0.00268
20	"	"	0.00088
40	"	"	0.00045
60	"	"	0.00033
0	6.5	0.436	0.11275
10	"	"	0.00268
20	"	"	0.00088
40	"	"	0.00045
60	"	"	0.00033

*Data are valid for "Low" pre-amplifier setting on the experimental receiver cover. For "Medium" setting, multiply values by 10. Setting "High" is not recommended.

Data corrected for the following "dark current" amplifier outputs:

"Low" pre-amplifier setting = -0.00075 volt

"Medium" pre-amplifier setting = -0.00650 volt

Table A-3. Results of Experimental Transmissometer Calibration.

Transmitter Angle (degrees)	Receiver Angle (degrees)	Interference Filter (μm)	Photocell* Amplifier Output (Corrected) (v)
0	2.0	0.656	0.24375
10	"	"	0.00820
20	"	"	0.00303
30	"	"	0.00180
40	"	"	0.00140
50	"	"	0.00114
60	"	"	0.00097
0	4.0	0.656	0.32075
10	"	"	0.01095
20	"	"	0.00425
40	"	"	0.00200
60	"	"	0.00138
0	6.5	0.656	0.33575
10	"	"	0.01145
20	"	"	0.00440
40	"	"	0.00200
60	"	"	0.00138

*Data are valid for "Low" pre-amplifier setting on the experimental receiver cover. For "Medium" setting, multiply values by 10. Setting "High" is not recommended.

Data corrected for the following "dark current" amplifier outputs:

"Low" pre-amplifier setting = -0.00075 volt

"Medium" pre-amplifier setting = -0.00650 volt

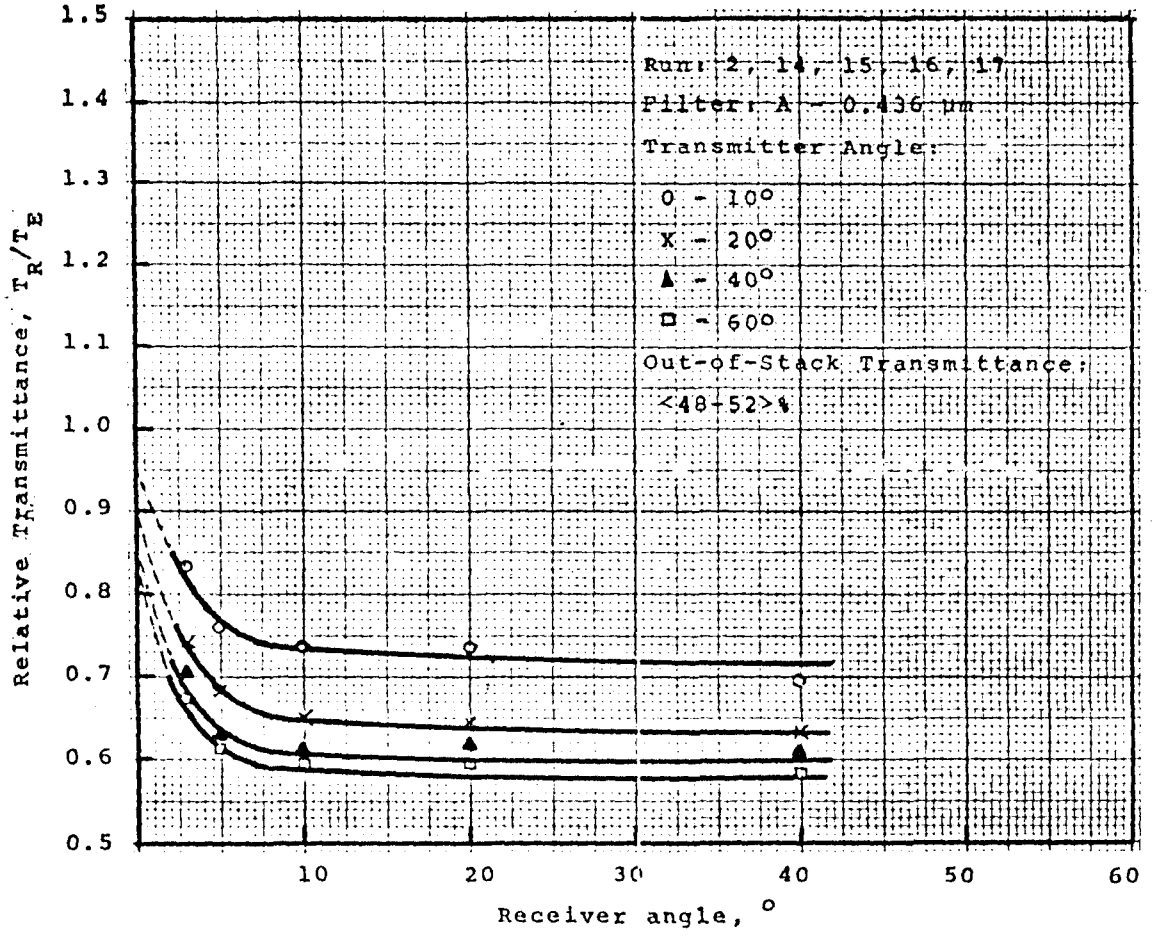

Figure A-1. Relationship of the Relative Transmittance and the Receiver and Transmitter Angle for 0.436μm Interference Filter.

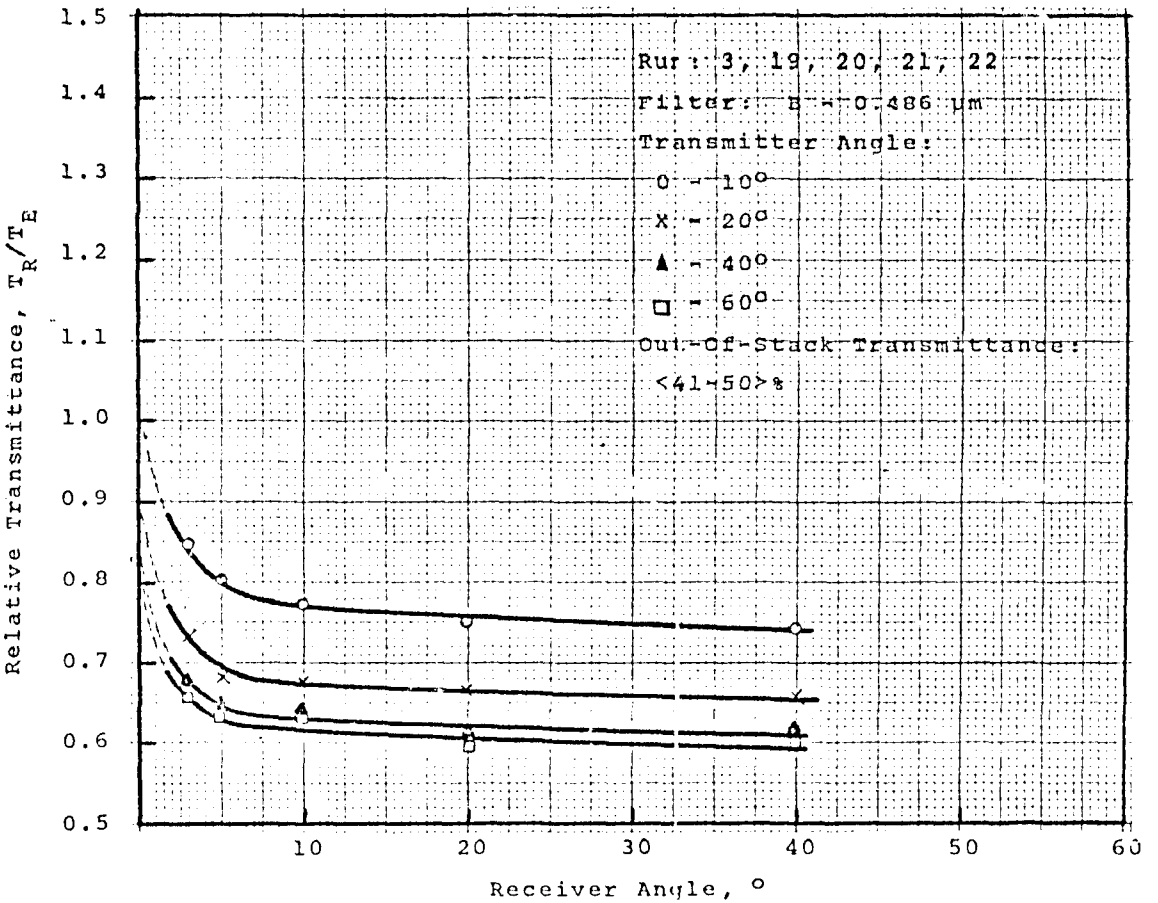

Figure A-2. Relationship of the Relative Transmittance and the Receiver and Transmitter Angle for 0.486μm Interference Filter.

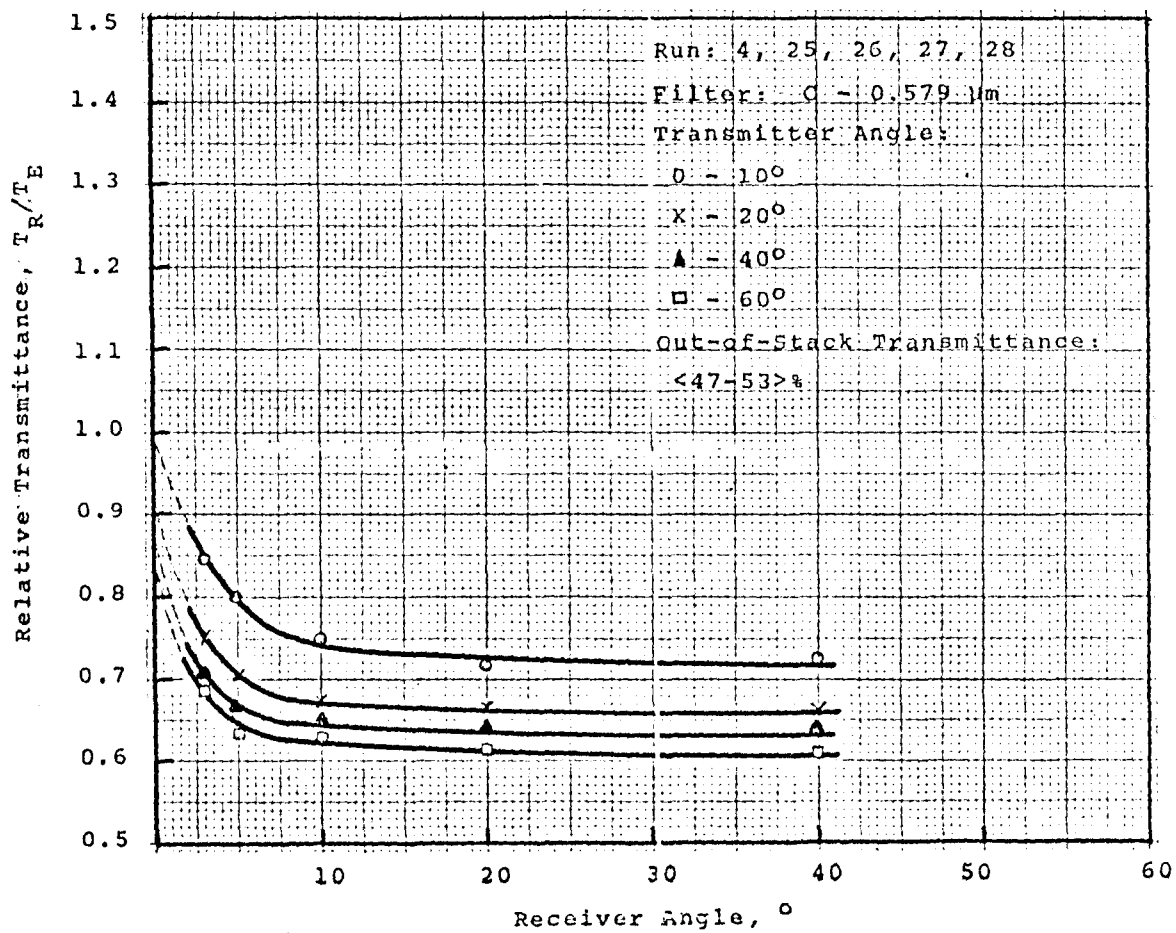

Figure A-3. Relationship of the Relative Transmittance and the Receiver and Transmitter Angle for 0.579μm Interference Filter.

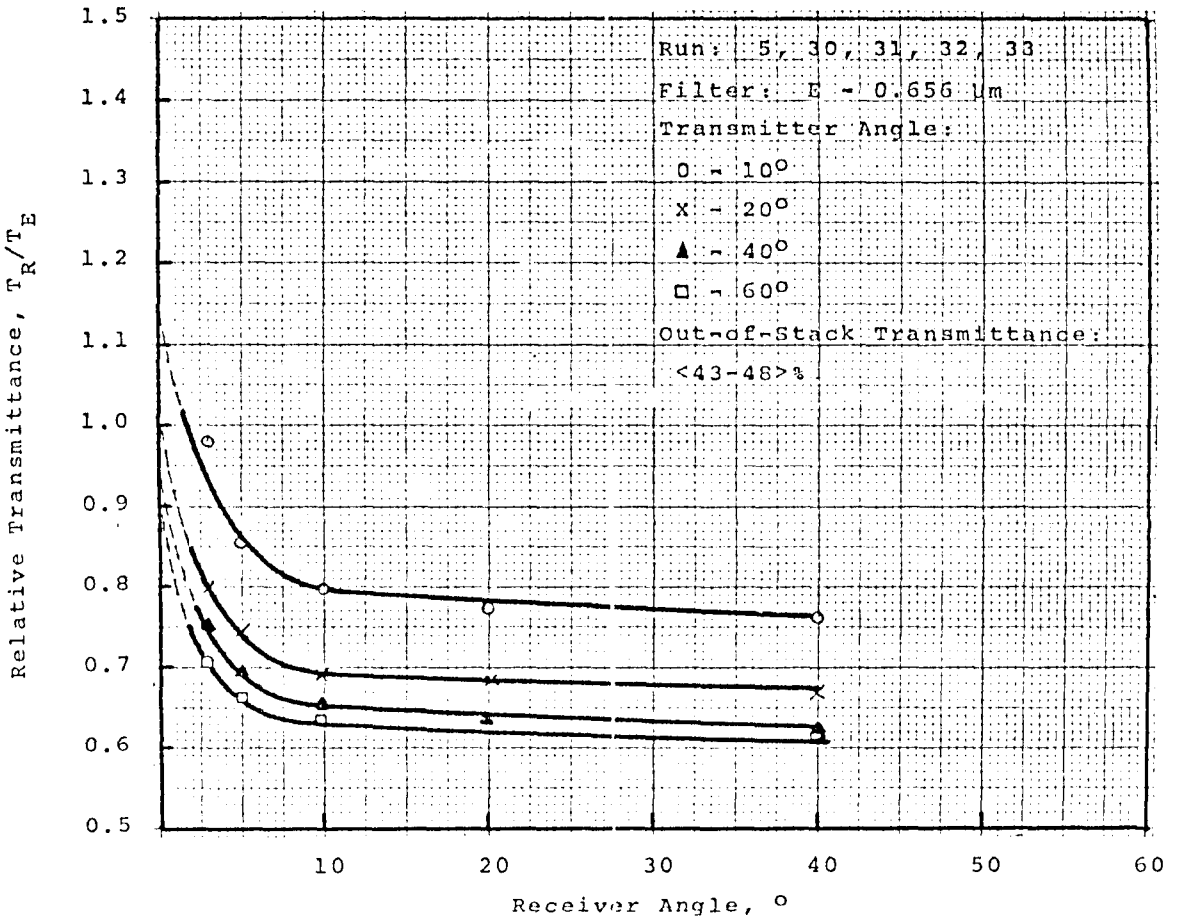

Figure A-4. Relationship of the Relative Transmittance and the Receiver and Transmitter Angle for 0.656µm Interference Filter.

The results can be summarized as follows:

1. The plots show the dependence of the in-stack transmittance on wavelength as already described in Section VIII.

2. The closest agreement between in-stack and plume transmittance measurements are achieved when either white light or interference filter between 0.486 and 0.579 micron are used.

3. The trend for the difference between the measured experimental transmittance and reference or plume transmittance to become greater for generally decreasing stack gas transmittance was also seen in this set of data. The difference becomes more evident for all cases when the data of Figure 13 of the main report (no filter) is replotted in the same dimensionless transmittance format as Figures A-1 through A-4 (filter data). The data of Figure 13 of the main report is presented in terms of the relative transmittance in Figure A-5. The results shown in Figures A-1 through A-4 were obtained when the plume transmittance was generally around 45 percent, whereas the data for Figure A-5 (no filter) was obtained at 60 to 80 percent transmittance.

Tabulated Experimental Data

The representative data collected throughout the experiments are presented for possible further evaluation in the following tables. Tables A-4 through A-7 contain the data obtained when no interference filters were used. Tables A-8 and A-9 were generated when a 0.436 micron filter was used. Data obtained while using 0.486, 0.579 and 0.656 are respectively presented in Tables A-10, A-11, A-12, A-13, A-14 and A-15.

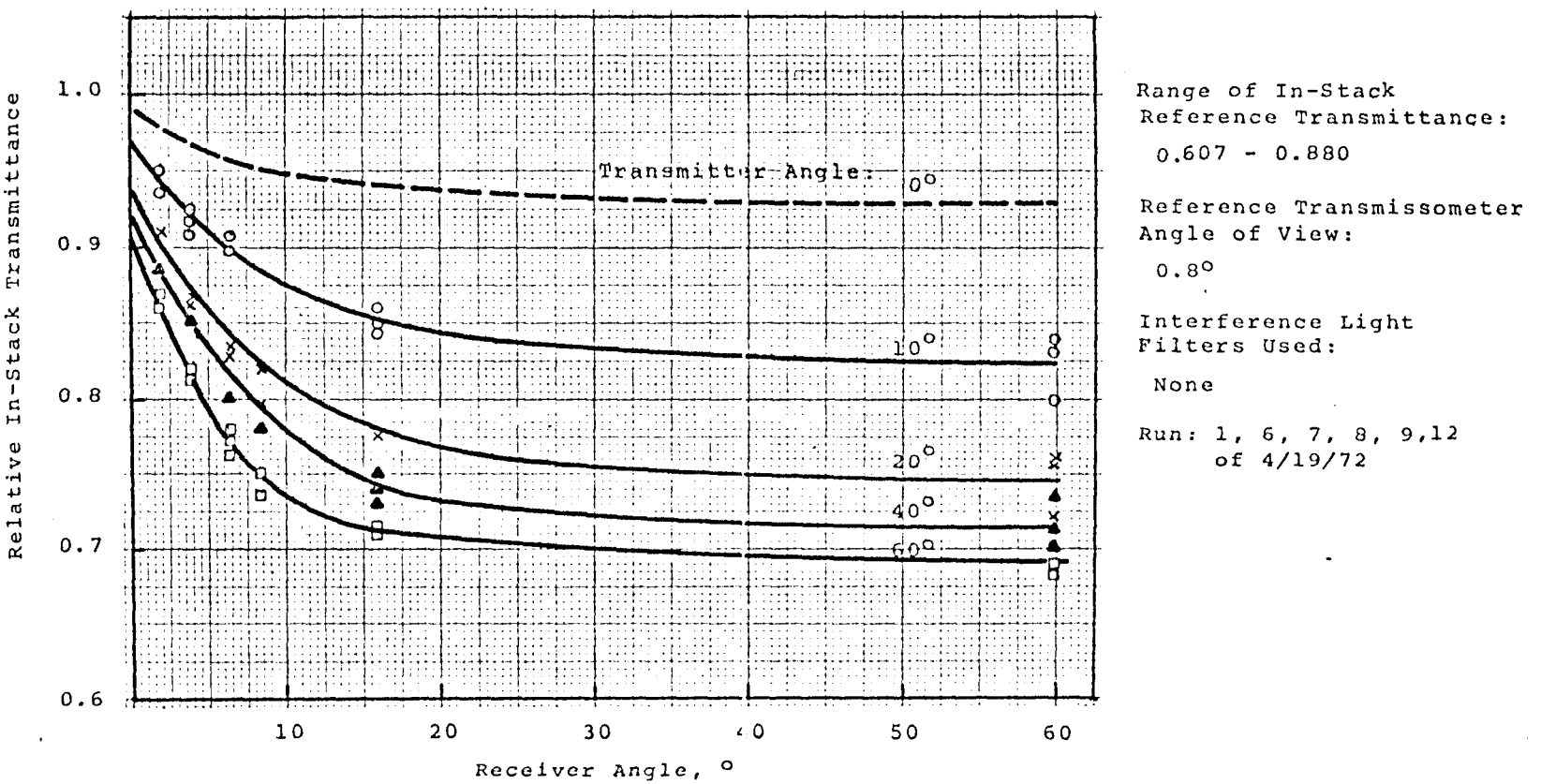

Figure A-5. The Receiver and Transmitter Angle Influence on the Relative In-Stack Transmittance Expressed as a Ratio of the Reference In-Stack Transmittance and of the Transmittance Measured by the Experimental Transmissometer for Given Receiver and Transmitter Angles.

Table A-4. In-Stack Transmissometer Field Results.

Run	Reference Transmittance	Experimental Transmitter Angle, °	Experimental Receiver Angle, °	Interference Filter, μm	Experimental Receiver Range	Corrected Zero Condition, No Aerosol Experimental Trans. Output, v	Experimental Transmissometer Output, v	Corrected Experimental Transmissometer Output, v	Experimental Transmittance	Dimensionless In-Stack Transmittance	Normalized Experimental Transmittance
1	2	3	4	5	6	7	8	9	10	11	12
1	0.612	10	2	N*	L*	0.26475	0.169	0.17075	0.645	0.948	0.851
1	0.607	10	2	N	L	0.26475	0.170	0.17175	0.649	0.936	0.882
1	0.744	20	2	N	L	0.09825	0.0785	0.08025	0.817	0.911	0.886
1	0.723	20	2	N	L	0.09825	0.078	0.07975	0.812	0.891	0.905
1	0.744	40	2	N	L	0.04925	0.0395	0.04125	0.837	0.888	0.909
1	0.744	60	2	N	L	0.03555	0.0286	0.03035	0.854	0.871	0.926
1	0.752	60	2	N	L	0.03555	0.0293	0.03105	0.873	0.861	0.937
7	0.764	10	4	N	L	0.3217	0.264	0.26575	0.826	0.925	0.872
7	0.744	10	4	N	L	0.32175	0.259	0.26075	0.810	0.918	0.879
7	0.764	10	4	N	L	0.32175	0.269	0.27075	0.841	0.908	0.889
7	0.793	20	4	N	L	0.12575	0.113	0.11475	0.912	0.869	0.929
7	0.785	20	4	N	L	0.12575	0.113	0.11475	0.912	0.860	0.938
7	0.773	20	4	N	L	0.12575	0.111	0.11275	0.897	0.862	0.936
7	0.859	40	4	N	L	0.06475	0.0637	0.06545	1.011	0.850	0.949
7	0.826	60	4	N	L	0.04575	0.0443	0.04645	1.006	0.821	0.983
7	0.806	60	4	N	L	0.04575	0.0436	0.04535	0.991	0.813	0.993

*N = No Filter; L = Low preamplifier setting.

Table A-5. In-Stack Transmissometer Field Results.

Run	Reference Transmittance	Experimental Transmitter Angle, °	Experimental Receiver Angle, °	Interference Filter, μm	Experimental Receiver Range	Corrected Zero Condition, No Aerosol Experimental Trans. Output, v	Experimental Transmissometer Output, v	Corrected Experimental Transmissometer Output, v	Experimental Transmittance	Dimensionless In-Stack Transmittance	Normalized Experimental Transmittance
1	2	3	4	5	6	7	8	9	10	11	12
6	0.859	10	6.5	N *	L *	0.33875	0.317	0.31875	0.948	0.908	0.889
6	0.826	10	6.5	N	L	0.33675	0.308	0.30975	0.920	0.898	0.889
6	0.847	20	6.5	N	L	0.13375	0.134	0.13575	1.015	0.835	0.966
6	0.859	20	6.5	N	L	0.13375	0.137	0.13875	1.037	0.828	0.975
6	0.859	40	6.5	N	L	0.06725	0.0706	0.07235	1.078	0.799	1.010
6	0.806	60	6.5	N	L	0.04775	0.0476	0.04935	1.033	0.780	1.035
6	0.859	60	6.5	N	L	0.04775	0.0514	0.05315	1.113	0.772	1.045
6	0.847	60	6.5	N	L	0.04775	0.051	0.05315	1.113	0.761	1.060
8	0.830	10	8.5	N	L	0.34175	0.322	0.32375	0.947	0.877	0.920
8	0.839	20	8.5	N	L	0.13375	0.135	0.13675	1.022	0.820	0.984
8	0.826	20	8.5	N	L	0.13375	0.137	0.13875	1.037	0.797	1.012
8	0.818	40	8.5	N	L	0.06725	0.0687	0.07045	1.047	0.781	1.033
8	0.835	60	8.5	N	L	0.04775	0.0514	0.05315	1.113	0.750	1.076
8	0.847	60	8.5	N	L	0.04775	0.0531	0.05485	1.149	0.737	1.095

*N = No filter; L = Low preamplifier setting.

Table A-6. In-Stack Transmissometer Field Results.

Run	Reference Transmittance	Experimental Transmitter Angle, °	Experimental Receiver Angle, °	Interference Filter, μm	Experimental Receiver Range	Corrected Zero Condition, No Aerosol Experimental Trans. Output, v	Experimental Transmissometer Output, v	Corrected Experimental Transmissometer Output, v	Experimental Transmittance	Dimensionless In-Stack Transmittance	Normalized Experimental Transmittance
1	2	3	4	5	6	7	8	9	10	11	12
9	0.810	10	16	N *	L*	0.33675	0.315	0.31675	0.941	0.861	0.937
9	0.802	10	16	N	L	0.33675	0.316	0.31775	0.944	0.850	0.949
9	0.822	10	16	N	L	0.33675	0.327	0.32675	0.976	0.842	0.958
9	0.835	20	16	N	L	0.13075	0.139	0.14075	1.076	0.775	1.041
9	0.855	40	16	N	L	0.06725	0.0769	0.07865	1.169	0.731	1.104
9	0.826	40	16	N	L	0.06725	0.0721	0.07385	1.098	0.752	1.073
9	0.847	40	16	N	L	0.06725	0.0751	0.07685	1.143	0.741	1.089
9	0.814	60	16	N	L	0.04795	0.0534	0.05515	1.150	0.708	1.140
9	0.806	60	16	N	L	0.04795	0.0527	0.05445	1.135	0.710	1.137

*N = No filter; L = Low preamplifier setting.

Table A-7. In-Stack Transmissometer Field Results.

Run	Reference Transmittance	Experimental Transmitter Angle, °	Experimental Receiver Angle, °	Interference Filter, μm	Experimental Receiver Range	Corrected Zero Condition, No Aerosol Experimental Trans. Output, v	Experimental Transmissometer Output, v	Corrected Experimental Transmissometer Output, v	Experimental Transmittance	Dimensionless In-Stack Transmittance	Normalized Experimental Transmittance
1	2	3	4	5	6	7	8	9	10	11	12
12	0.806	10	60	N*	L*	0.33675	0.338	0.33975	1.009	0.798	1.011
12	0.797	10	60	N	L	0.33675	0.322	0.32375	0.961	0.830	0.972
12	0.835	10	60	N	L	0.33675	0.332	0.33375	0.991	0.842	0.958
12	0.806	20	60	N	L	0.13075	0.138	0.13975	1.069	0.754	1.070
12	0.868	20	60	N	L	0.13075	0.155	0.15675	1.199	0.724	1.115
12	0.818	20	60	N	L	0.13075	0.139	0.14075	1.076	0.760	1.062
12	0.847	40	60	N	L	0.06725	0.0757	0.07745	1.152	0.735	1.098
12	0.868	40	60	N	L	0.06725	0.0816	0.08335	1.239	0.700	1.153
12	0.880	40	60	N	L	0.06725	0.0814	0.08315	1.236	0.712	1.133
12	0.797	60	60	N	L	0.04795	0.0542	0.05595	1.167	0.683	1.181
12	0.814	60	60	N	L	0.04795	0.0548	0.05655	1.179	0.690	1.169

*N = No filter; L = Low preamplifier setting

Table A-8. In-Stack Transmissometer Field Results.

Run	Reference Transmittance	Experimental Transmitter Angle, °	Experimental Receiver Angle, °	Interference Filter, μm	Experimental Receiver Range	Corrected Zero Condition, No Aerosol Experimental Trans. Output, v	Experimental Transmissometer Output, v	Corrected Experimental Transmissometer Output, v	Experimental Transmittance	Dimensionless In-Stack Transmittance	Normalized Experimental Transmittance	Corrected Dimensionless Transmittance
1	2	3	4	5	6	7	8	9	10	11	12	13
2a	0.562	0	3	A*	M*	0.4918	0.223	0.247	0.502	1.12		1.064
2b	0.562	10	3	A	M	0.0419	0.00276	0.02676	0.639	0.88		0.836
2c	0.562	20	3	A	M	0.242	-0.00656	0.01744	0.721	0.78		0.741
2d	0.562	40	3	A	M	0.0202	-0.00823	0.01577	0.781	0.74		0.703
2e	0.562	60	3	A	M	0.0193	-0.00883	0.01517	0.786	0.71		0.674
14a	0.562	0	5	A	M	1.2689	0.696	0.720	0.567	0.99		0.940
14b	0.547	10	5	A	M	0.0509	0.0107	0.0347	0.662	0.80		0.760
14c	0.531	20	5	A	M	0.027[illegible]	-0.00387	0.02013	0.743	0.715		0.681
14d	0.541	40	5	A	M	0.0216	-0.00629	0.01771	0.820	0.66		0.627
14e	0.531	60	5	A	M	0.0202	-0.00762	0.01638	0.811	0.65		0.617
15a	0.531	0	10	A	M	1.3049	0.721	0.745	0.571	0.93		0.883
15b	0.531	10	10	A	M	0.0509	0.0106	0.0346	0.680	0.78		0.741
15c	0.531	20	10	A	M	0.0274	-0.00276	0.02124	0.775	0.685		0.650
15d	0.531	40	10	A	M	0.0218	-0.00605	0.01795	0.823	0.64		0.608
15e	0.531	60	10	A	M	0.0203	-0.00689	0.01714	0.844	0.63		0.598

*A = 0.436 μm interference filter; M = Medium preamplifier setting.

Table A-9. In-Stack Transmissometer Field Results.

Run	Reference Transmittance	Experimental Transmitter Angle, °	Experimental Receiver Angle, °	Interference Filter, μm	Experimental Receiver Range	Corrected Zero Condition, No Aerosol Experimental Trans. Output, v	Experimental Transmissometer Output, v	Corrected Experimental Transmissometer Output, v	Experimental Transmittance	Dimensionless In-Stack Transmittance	Normalized Experimental Transmittance	Corrected Dimensionless Transmittance
1	2	3	4	5	6	7	8	9	10	11	12	13
16a	0.531	0	20	A *	M*	1.3049	0.748	0.772	0.591	0.90		0.855
16b	0.562	10	20	A	M	0.0509	0.0127	0.0367	0.721	0.78		0.741
16c	0.531	20	20	A	M	0.0274	-0.00260	0.0214	0.781	0.68		0.646
16d	0.531	40	20	A	M	0.0218	-0.00633	0.01767	0.810	0.65		0.617
16e	0.541	60	20	A	M	0.0203	-0.00657	0.01743	0.859	0.63		0.598
17a	0.541	0	40	A	M	1.3049	0.756	0.780	0.598	0.90		0.855
17b	0.525	10	40	A	M	0.0509	0.011	0.0366	0.719	0.73		0.693
17c	0.531	20	40	A	M	0.0274	-0.00228	0.02172	0.793	0.67		0.636
17d	0.553	40	40	A	M	0.0218	-0.00531	0.01869	0.857	0.64		0.608
17e	0.541	60	40	A	M	0.0203	-0.00629	0.01771	0.872	0.62		0.589

*A = 0.436 μm interference filter; M = Medium preamplifier setting

Table A-10. In-Stack Transmissometer Field Results.

Run	Reference Transmittance	Experimental Transmitter Angle, °	Experimental Receiver Angle, °	Interference Filter, μm	Experimental Receiver Range	Corrected Zero Condition, No Aerosol Experimental Trans. Output, v	Experimental Transmissometer Output, v	Corrected Experimental Transmissometer Output, v	Experimental Transmittance	Dimensionless In-Stack Transmittance	Normalized Experimental Transmittance	Corrected Dimensionless Transmittance
1	2	3	4	5	6	7	8	9	10	11	12	13
3a	0.537	0	3	B *	M*	2.8869	1.27	1.29	0.448	1.12		1.064
3b	0.525	10	3	B	M	0.0798	0.0231	0.0471	0.590	0.89		0.845
3c	0.541	20	3	B	M	0.0356	0.0010	0.0250	0.702	0.77		0.731
3d	0.547	40	3	B	M	0.0271	-0.00312	0.02088	0.770	0.71		0.674
3e	0.537	60	3	B	M	0.0240	-0.00532	0.01868	0.778	0.69		0.655
19a	0.528	0	5	B	M	3.3709	1.65	1.67	0.497	1.06		1.007
19b	0.531	10	5	B	M	0.1023	0.0477	0.0643	0.628	0.84		0.798
19c	0.547	20	5	B	M	0.0130	0.00822	0.03222	0.749	0.73		0.693
19d	0.541	40	5	B	M	0.0311	0.00074	0.02479	0.797	0.68		0.646
19e	0.531	60	5	B	M	0.0269	-0.00268	0.02132	0.792	0.67		0.636
20a	0.537	0	10	B	M	3.4692	1.83	1.85	0.531	1.01		0.959
20b	0.531	10	10	B	M	0.1033	0.043	0.067	0.648	0.82		0.779
20c	0.525	20	10	B	M	0.0436	0.00823	0.03223	0.739	0.71		0.674
20d	0.531	40	10	B	M	0.0318	0.0012	0.0252	0.792	0.67		0.636
20e	0.531	60	10	B	M	0.0273	-0.0022	0.0218	0.798	0.66		0.627

*B = 0.486 μm interference filter; M = Medium preamplifier setting.

Table A-11. In-Stack Transmissometer Field Results.

Run	Reference Transmittance	Experimental Transmitter Angle, o	Experimental Receiver Angle, o	Interference Filter, μm	Experimental Receiver Range	Corrected Zero Condition, No Aerosol Experimental Trans. Output, v	Experimental Transmissometer Output, v	Corrected Experimental Transmissometer Output, v	Experimental Transmittance	Dimensionless In-Stack Transmittance	Normalized Experimental Transmittance	Corrected Dimensionless Transmittance
1	2	3	4	5	6	7	8	9	10	11	12	13
21a	0.547	0	20	B*	M*	3.4692	1.93	1.95	0.563	0.97		0.921
21b	0.531	10	20	B	M	0.1033	0.0454	0.0694	0.672	0.79		0.750
21c	0.547	20	20	B	M	0.0436	0.0100	0.0340	0.780	0.70		0.665
21d	0.531	40	20	B	M	0.0318	0.00158	0.02558	0.804	0.66		0.627
21e	0.531	60	20	B	M	0.0273	-0.00099	0.02301	0.843	0.63		0.598
22a	0.469	0	40	B	M	3.4692	1.69	1.71	0.494	0.95		0.902
22b	0.469	10	40	B	M	0.1033	0.038	0.062	0.600	0.78		0.741
22c	0.469	20	40	B	M	0.0436	0.00563	0.02963	0.679	0.69		0.655
22d	0.469	40	40	B	M	0.0318	-0.00105	0.02295	0.722	0.65		0.617
22e	0.469	60	40	B	M	0.0273	-0.0040	0.0200	0.733	0.64		0.608

*B = 0.486 μm interference filter; M = Medium preamplifier setting.

Table A-12. In-Stack Transmissometer Field Results.

Run	Reference Transmittance	Experimental Transmitter Angle, °	Experimental Receiver Angle, °	Interference Filter, μm	Experimental Receiver Range	Corrected Zero Condition, No Aerosol Experimental Trans. Output, v	Experimental Transmissometer Output, v	Corrected Experimental Transmissometer Output, v	Experimental Transmittance	Dimensionless In-Stack Transmittance	Normalized Experimental Transmittance	Corrected Dimensionless Transmittance
1	2	3	4	5	6	7	8	9	10	11	12	13
4a	0.566	0	3	C*	M*	0.3292	0.121	0.145	0.440	1.28		1.216
4b	0.566	10	3	C	M	0.1285	0.0572	0.0812	0.632	0.89		0.845
4c	0.573	20	3	C	M	0.0530	0.0145	0.0385	0.726	0.79		0.750
4d	0.573	40	3	C	M	0.0345	0.00266	0.02666	0.773	0.74		0.703
4e	0.576	60	3	C	M	0.0294	-0.00052	0.02348	0.799	0.72		0.684
25a	0.533	0	5	C	M	6.0439	2.75	2.77	0.459	1.16		1.102
25b	0.533	10	5	C	M	0.1684	0.083	0.107	0.635	0.84		0.798
25c	0.533	20	5	C	M	0.0613	0.0244	0.0484	0.720	0.74		0.703
25d	0.533	40	5	C	M	0.0414	0.0076	0.0316	0.763	0.70		0.665
25e	0.533	60	5	C	M	0.0344	0.0035	0.0275	0.799	0.67		0.636
26a	0.533	0	10	C	M	6.2209	2.99	3.014	0.484	1.10		1.045
26b	0.533	10	10	C	M	0.1701	0.090	0.114	0.670	0.79		0.750
26c	0.533	20	10	C	M	0.0683	0.0273	0.0513	0.751	0.71		0.674
26d	0.533	40	10	C	M	0.0426	0.0090	0.0330	0.775	0.69		0.655
26e	0.533	60	10	C	M	0.0350	0.00422	0.02822	0.806	0.66		0.627

*C = 0.579 μm interference filter; M = Medium preamplifier setting

Table A-13. In-Stack Transmissometer Field Results.

Run	Reference Transmittance	Experimental Transmitter Angle, °	Experimental Receiver Angle, °	Interference Filter, μm	Experimental Receiver Range	Corrected Zero Condition, No Aerosol Experimental Trans. Output, v	Experimental Transmissometer Output, v	Corrected Experimental Transmissometer Output, v	Experimental Transmittance	Dimensionless In-Stack Transmittance	Normalized Experimental Transmittance	Corrected Dimensionless Transmittance
1	2	3	4	5	6	7	8	9	10	11	12	13
27a	0.540	0	20	C *	M*	6.2209	3.27	3.294	0.529	1.02		0.969
27b	0.533	10	20	C	M	0.1701	0.0966	0.1206	0.709	0.75		0.712
27c	0.533	20	20	C	M	0.0683	0.0280	0.0520	0.761	0.70		0.665
27d	0.533	40	20	C	M	0.0426	0.0093	0.0333	0.782	0.68		0.646
27e	0.533	60	20	C	M	0.0350	0.00445	0.02845	0.813	0.65		0.617
28a	0.533	0	40	C	M	6.2209	3.27	3.294	0.529	1.00		0.950
28b	0.533	10	40	C	M	0.1701	0.0949	0.1189	0.699	0.76		0.722
28c	0.533	20	40	C	M	0.0683	0.0284	0.0524	0.767	0.695		0.660
28d	0.533	40	40	C	M	0.0426	0.00928	0.03328	0.781	0.68		0.646
28e	0.533	60	40	C	M	0.0350	0.00492	0.02892	0.826	0.64		0.608

*C = 0.579 μm interference filter; M = Medium preamplifier setting.

Table A-14. In-Stack Transmissometer Field Results.

Run	Reference Transmittance	Experimental Transmitter Angle, °	Experimental Receiver Angle, °	Interference Filter, μm	Experimental Receiver Range	Corrected Zero Condition, No Aerosol Experimental Trans. Output, v	Experimental Transmissometer Output, v	Corrected Experimental Transmissometer Output, v	Experimental Transmittance	Dimensionless In-Stack Transmittance	Normalized Experimental Transmittance	Corrected Dimensionless Transmittance
1	2	3	4	5	6	7	8	9	10	11	12	13
5a	0.531	0	3	E*	M*	4.7159	1.54	1.564	0.332	1.6		1.52
5b	0.531	10	3	E	M	0.1151	0.035	0.059	0.512	1.03		0.978
5c	0.534	20	3	E	M	0.0500	0.00797	0.03197	0.639	0.835		0.793
5d	0.531	40	3	E	M	0.0339	-0.00135	0.02265	0.668	0.79		0.75
5e	0.531	60	3	E	M	0.0296	-0.0029	0.02110	0.713	0.74		0.703
30a	0.500	0	5	E	M	5.5069	1.88	1.904	0.346	1.45		1.38
30b	0.516	10	5	E	M	0.1499	0.0617	0.0857	0.572	0.90		0.855
30c	0.506	20	5	E	M	0.06[illegible]	0.0169	0.04090	0.648	0.78		0.741
30d	0.516	40	5	E	M	0.0407	0.00469	0.02869	0.705	0.73		0.693
30e	0.516	60	5	E	M	0.0346	0.00132	0.02532	0.732	0.70		0.665
31a	0.475	0	10	E	M	5.6679	2.03	2.054	0.362	1.31		1.244
31b	0.475	10	10	E	M	0.1519	0.0614	0.0854	0.562	0.84		0.796
31c	0.494	20	10	E	M	0.0641	0.0194	0.0434	0.677	0.73		0.693
31d	0.484	40	10	E	M	0.0418	0.00511	0.02911	0.696	0.69		0.655
31e	0.500	60	10	E	M	0.0353	0.00215	0.02615	0.741	0.67		0.636

*E = 0.656 μm interference filter; M = Medium preamplifier setting.

Table A-15. In-Stack Transmissometer Field Results.

Run	Reference Transmittance	Experimental Transmitter Angle, °	Experimental Receiver Angle, °	Interference Filter, μm	Experimental Receiver Range	Corrected Zero Condition, No Aerosol Experimental Trans. Output, v	Experimental Transmissometer Output, v	Corrected Experimental Transmissometer Output, v	Experimental Transmittance	Dimensionless In-Stack Transmittance	Normalized Experimental Transmittance	Corrected Dimensionless Transmittance
1	2	3	4	5	6	7	8	9	10	11	12	13
32a	0.500	0	20	E*	M*	5.6679	2.19	2.214	0.390	1.28		1.216
32b	0.500	10	20	E	M	0.1519	0.0685	0.0925	0.610	0.82		0.779
32c	0.500	20	20	E	M	0.0641	0.0205	0.0445	0.694	0.72		0.684
32d	0.500	40	20	E	M	0.0418	0.00696	0.03096	0.741	0.67		0.636
32e	0.500	60	20	E	M	0.0353	0.00226	0.02626	0.744	0.67		0.636
33a	0.462	0	40	E	M	5.6679	2.100	2.124	0.375	1.23		1.168
33b	0.500	10	40	E	M	0.1519	0.0704	0.0944	0.621	0.80		0.760
33c	0.500	20	40	E	M	0.0641	0.0211	0.0451	0.703	0.71		0.674
33d	0.516	40	40	E	M	0.0418	0.00848	0.03248	0.777	0.66		0.627
33e	0.484	60	40	E	M	0.0353	0.00189	0.02589	0.733	0.65		0.617

*E = 0.656 μm interference filter; M = Medium preamplifier setting.

APPENDIX B

NOTES TO THE REFERENCE AND EXPERIMENTAL TRANSMISSOMETER OPERATION

Electrical Hookup and Alignment of the Instruments

Both transmissometers operate on 115 volts A.C., 60 Hz, connected to the transmitter housing by a twist-type electrical plug. While operating, the transmitter and receiver must be interconnected by a shielded cable (about 15 feet long) supplied with the instruments. The amplifier output signal is available from a ampheral plug on the side of the transmitter housing and can be transmitted through about 50 feet of shielded cable to any high input impedance voltmeter. The range of the readout for the reference transmissometer should be from 0 to about 0.5 volt depending on the optical distance of the transmitter and receiver. The range for the experimental transmissometer should be from -0.001 to +7.0 volt.

After about 30 minutes warmup period, the power supply voltage for the transmitter lamp must be adjusted to 8.0 volts on the experimental transmitter, and 6.5 volts on the reference transmitter. The voltage should be measured on the lamp socket of the reference transmitter that is accessible after removing the cover. After attaching measurement probes, the voltage must be checked with the cover closed so as not to influence the lamp control photoelectric circuit. Two lamp voltage terminals are provided on an outside panel of the experimental transmitter housing and the cover of the experimental transmitter does not have to be opened during the lamp voltage check.

The lamp voltage can be adjusted in each instrument by adjusting a trimmer that is labeled LAMP and which is accessible after removing the transmitter housing cover.

No other electrical alignment except the lamp voltage is required.

Suggested Optical Alignment

To align the instrument on the stack, the procedure described in Section III of this report should be followed.

Maintenance

No special maintenance of the reference transmissometer is required. When the instrument is operated on a negative pressure duct or stack, the lens protection system is sufficient to keep them clean for several hundreds of hours. The only maintenance may be the lamp replacement which can be easily done after opening the reference transmitter cover.

The experimental receiver lens requires checking and cleaning about every 80 hours of operation and the transmitter lens must be checked and, if necessary, cleaned once an hour.

When the instruments are to be used on a positive pressure duct or stack, a high pressure and possibly greater volume of clean flushing air to the optical system must be provided.

The lamp in the experimental transmitter is replaced by performing the following operations:

1) Remove the instrument housing cover.

2) Disconnect the cable leading from the lamp assembly to the electronic component.

3) Slide the lamp assembly out of the support tube housing.

4) Remove the flushing/cooling air base fitting from the lamp assembly.

5) Remove the lamp voltage control photocell located inside the lamp assembly tube.

6) Loosen the three set-screws at the base of the lamp socket.

7) Turn and lift out lamp.

The new lamp may be installed and the instrument re-assembled by following the described lamp removal process in reverse.

Electrical Diagrams

The electrical diagrams of the experimental and reference transmissometers shown in Figures B-1 and B-2 are enclosed for ease in trouble-shooting in the event that electrical malfunction occurs.

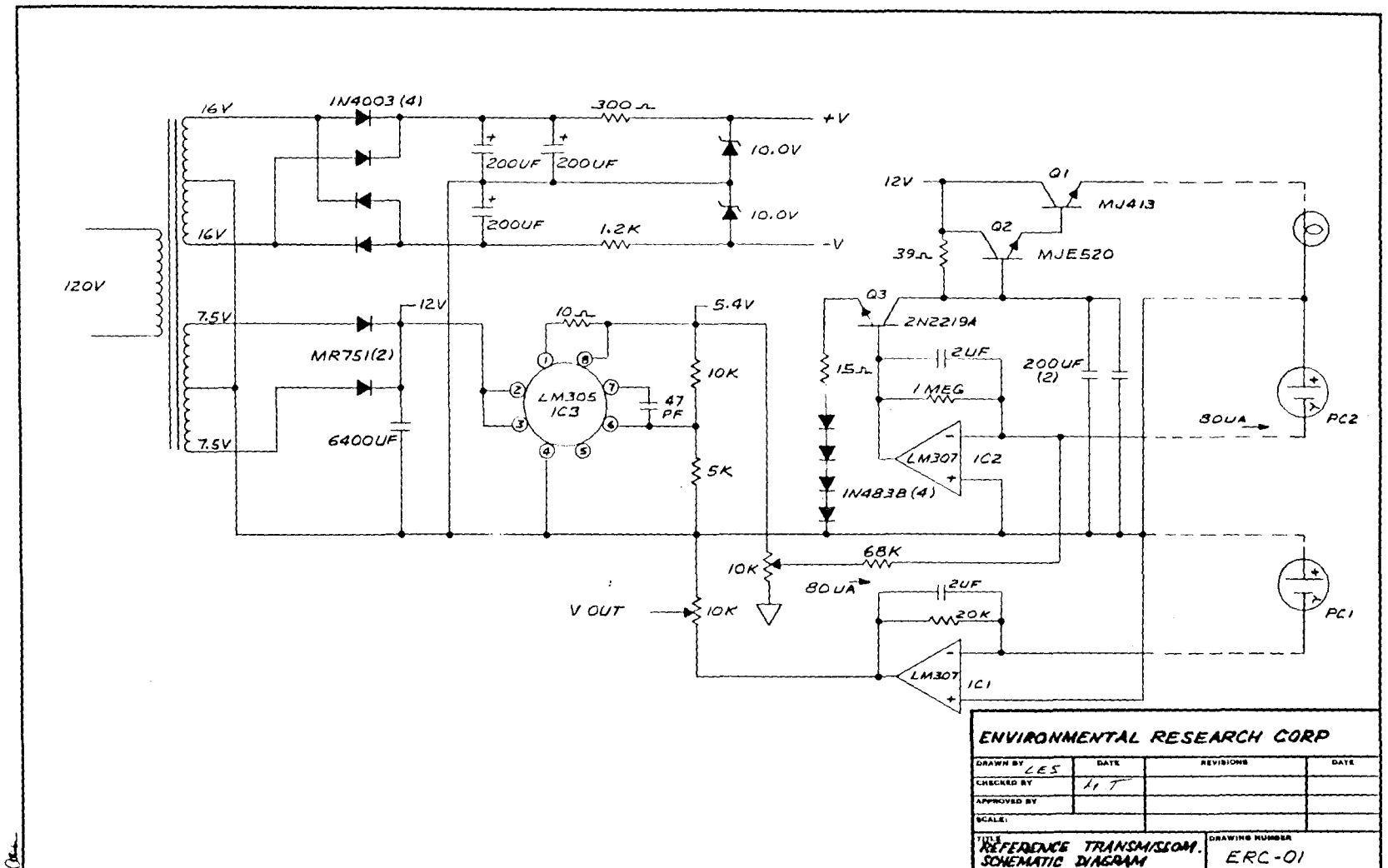

Figure B-1. Reference Transmissometer Wiring Diagram.

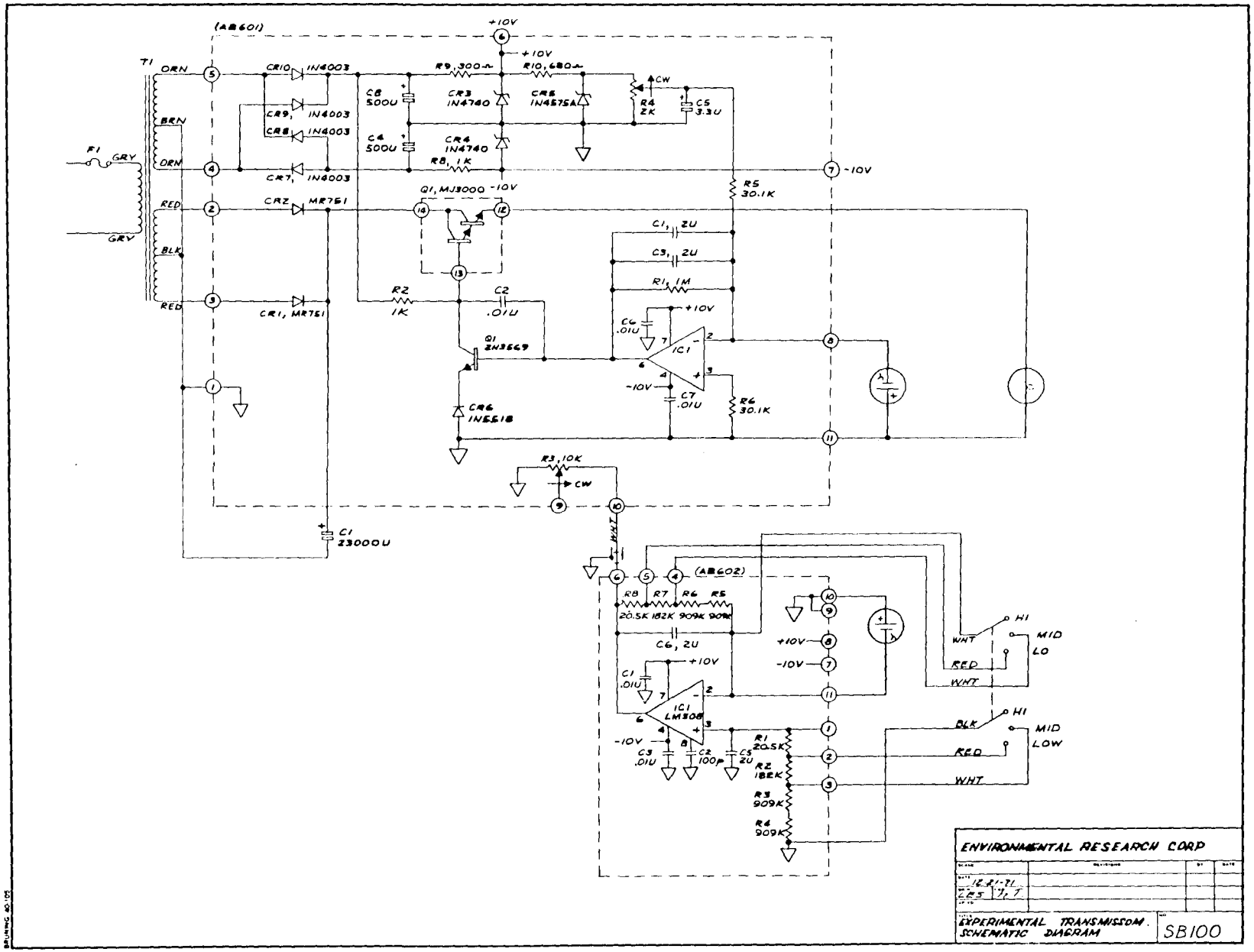

Figure B-2. Experimental Transmissometer Wiring Diagram.